A comparative analysis of Urban Vulnerability using a Geographical Information System based on fuzzy Multi-Criteria Dimensional Analysis in The Metropolitan Region of the Hooghly River Delta and the Chao Phraya River Delta.

A thesis

Submitted in partial fulfilment of the requirements for the award of the degree of

M. Tech in Environmental Biotechnology

Jadavpur University

By

Ankita Das

Environmental Biotechnology

Roll Number: 002230904012

Registration Number: 163793 of 2022-2023

Exam Roll Number: M4EBT24007

Under the supervision of

Dr. Reshmi Das

UGC Assistant Professor

School of Environmental Studies

Faculty of Interdisciplinary Studies, Law and Management

Jadavpur University

Jadavpur, Kolkata-700032

DECLARATION

I hereby declare that the work presented in this thesis report titled **"A comparative analysis of Urban Vulnerability using Geographical Information System based on fuzzy Multi-Criteria Dimensional Analysis in the Metropolitan Region of the Hooghly River Delta and the Chao Phraya River Delta"** submitted to Jadavpur University, Kolkata- 32, in partial fulfilment of the requirements for the award of the degree of M. Tech is a bonafide record of the research work carried out under the supervision of Dr. Reshmi Das. The contents of the Thesis report in parts, have not been submitted to and will not be submitted by me to any other Institute or University in India or abroad for the award of any degree or diploma.

Ankita Das.

Signature

Ankita Das

Roll no.: 002230904012

Exam Roll No: M4EBT24007

Environmental Biotechnology

School of Environmental Studies

Jadavpur University, Kolkata- 32

CERTIFICATE

This is to certify that the Thesis Report titled **“A Comparative Analysis of Urban Vulnerability using Geographical Information System based on Fuzzy Multi-Criteria Dimensional Analysis in the Metropolitan Region of the Hooghly River Delta and the Chao Phraya River Delta”**, submitted by Ankita Das (002230904012) to Jadavpur University, Kolkata for the award of the degree of M. Tech, is a bonafide record of the research work done by her under my supervision. To the best of my knowledge, the constituents of this report, in full or in parts, have not been submitted to any other Institute or University for the award of any degree or diploma.

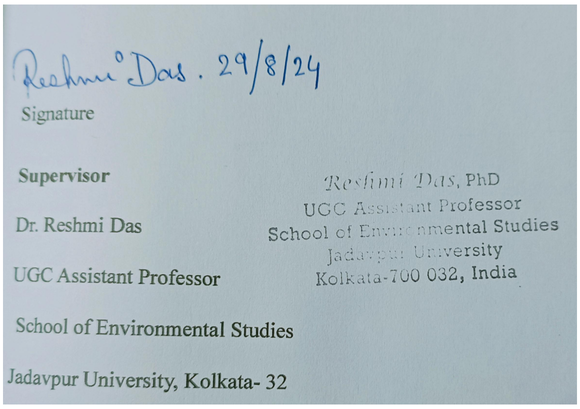

Reshmi Das. 29/8/24

Signature

Supervisor

Dr. Reshmi Das

UGC Assistant Professor

School of Environmental Studies

Jadavpur University, Kolkata- 32

Reshmi Das, PhD
UGC Assistant Professor
School of Environmental Studies
Jadavpur University
Kolkata-700 032, India

TO WHOM IT MAY CONCERN

It is hereby notified that this thesis titled "A Comparative Analysis of Urban Vulnerability Using Geographical Information System based on Fuzzy Multi-Criteria Dimensional Analysis in the Metropolitan Region of the Hooghly River Delta and the Chao Phraya River Delta", is prepared and submitted for the partial fulfilment of the continuous assessment of Master of Technology in Environmental Biotechnology course of Jadavpur University by Ankita Das (002230904012), a student of the said course for session 2022-2024. It is also declared that no part of this thesis has been presented or published elsewhere.

29/8/24

Director
School of Environmental Studies
JADAVPUR UNIVERSITY
Kolkata - 700 032

(Signature with Seal)

Director

Prof. Joydeep Mukherjee

School of Environmental Studies

Jadavpur University, Kolkata- 32

Reshmi Das 29/8/24

(Signature with Seal)

Thesis Supervisor

Dr. Reshmi Das

School of Environmental Studies

Jadavpur University, Kolkata- 32

Reshmi Das, PhD
UGC Assistant Professor
School of Environmental Studies
Jadavpur University
Kolkata-700 032, India

29/8/24

(Signature with Seal)

Dean, Faculty of Interdisciplinary Studies Law and Management

Jadavpur University, Kolkata- 32

DEAN
Faculty of Interdisciplinary Studies,
Law & Management
Jadavpur University

CERTIFICATE OF APPROVAL

This foregoing thesis is hereby approved as a credible study of an engineering subject carried out and presented in a manner satisfactorily to warrant its acceptance as a prerequisite to the degree for which it has been submitted. It is understood that by this approval the undersigned do not endorse or approve any statement made or opinion expressed or conclusion drawn therein but approve the thesis only for the purpose for which it has been submitted.

\-

Final examination for evaluation of the thesis

\-

Signature of the Examiners

ACKNOWLEDGMENT

I would like to extend my heartfelt appreciation to my supervisor, Dr. Reshmi Das, School of Environmental Studies, Jadavpur University, for her steadfast mentorship, motivation, and assistance during the entirety of my M. Tech research and study. Their extensive knowledge and patience have helped me with my studies and thesis writing. Along with my advisors, for support, encouragement, and advice, I would also like to thank Dr. Joydeep Mukherjee, School of Environmental Studies, Dr. Tarit Roy Chowdhury, School of Environmental Studies, and Dr. Subarna Bhattacharyya, School of Environmental Studies. I would also like to thank to all of the research scholars for their help, encouragement, and support during my M. Tech project work, especially to Kazi Hamidul Islam. My departmental peers have also helped me whenever I needed it, and I am grateful for that. Lastly, I would want to sincerely thank my parents for their inspiration and steadfast support during this time.

Ankita Das

ABSTRACT

Urban Vulnerabilities in the deltaic metropolitan areas have become a challenging concern, affected by seasonal variations and varied environmental socio-economical, and demographical factors. This study represents a comparative analysis of the Urban Vulnerability of two deltaic megacities namely Bangkok Metropolitan Region (BMR), Thailand, and Kolkata Metropolitan Area (KMA), India. This study employed Geographical Information System (GIS) based fuzzy Multi-Criteria Dimensional Analysis (MCDA) to map spatial data and assess vulnerabilities regarding parameters such as Rainfall, AQI, LST, NDBI, NDVI, Population Density, Old/Child Population, Literacy Rate, and Per Capita Income, focusing on how these parameters fluctuate with the summer, monsoon and winter season, and also its impacts in the metropolis due to seasonal variations. The results indicate that about 4.70 sq. km.(0.3%) and 585.23 sq. km.(37.3%) of the area in the central region and its surroundings of BMR and 21.50sq. km.(1.14%) and 68.29 sq. km.(3.62%) of the area in the central region and its surroundings of KMA are highly vulnerable in summer and monsoon and also highly exposed to multiple climatic and physiological threats, especially heat waves, cardiovascular disease, and neurological diseases. The study also highlights how elderly, children and low-income groups are more susceptible to vulnerabilities. The study explains the relationship between seasonal environmental shifts and physiological threats, stressing for the need of season-specific public health strategies and proper urban planning measures. To mitigate the effects of Urban Vulnerability in deltaic megacities, policymakers, and urban planners shall consider the findings of this study into account while planning sustainable solutions to the hazards.

Keywords – Urban Vulnerability; Urban Heat Island (UHI); Metropolis; Rainfall; AQI; LST; NDBI; NDVI; Urban sprawl

Table of Contents

List of Tables

List of Figures

Chapter 1: Introduction

1 Introduction

The growing demand for resources worsening the world's population expansion and ongoing development, puts additional stress on the planet's ecosystem (Tiwari, 2000). Due to greater access to employment, education, financial opportunities, and standard of living in metropolitan areas, people are relocating from rural areas. Urban areas are expanding physically faster than their rate of population, and by 2030 cities are projected to encompass thrice as much land as did in 2000, posing a threat to biodiversity hotspots area (Angel et al., 2011; Seto et al., 2010; Seto et al., 2012). Urban areas face the consequences of climate change, which has detrimental effects on environmental, social, demographical, and institutional issues, and health impacts. To overcome these factors, it is essential to develop sustainable ways to effectively govern urban growth (UN-Habitat, 2022). Repercussions of urbanization are changes in the pattern of Land Use Land Cover (LULC), decrease in vegetation index, air pollution, rise of sea level, increase in rainfall, increase in global temperature, severe droughts, floods, increase in frequency of cyclones, increase in building density, compromise of public health, inadequate excess to employment opportunities and education (IPCC, 2021).

United Nations estimated the world population in 2022 to be 8 billion and projected that the world population will rise to around 8.5 billion in 2030, 9.7 billion in 2050, and 10.4 billion in 2100, whereas South and Southeast Asia being the most populous region, nearly 1.4 billion people live in India and China in 2022 (World Population Prospects (WPP), 2022). IPCC, 2022 shows that about 332 million migrants settle in South and Southeast Asia, and the region's current population makes up 54% and is projected to rise 64% by 2050. With women and girls making up 49.7% of the world's population and men 50.3%, gender disparity puts them at risk for health problems as the population increases; with time, this statistic is estimated to gradually reverse, and by 2050, it is anticipated that the male and female populations will be almost equal

(WPP, 2022). Between 2015 and 2020, the urban population grew to 397 million mostly in less developed areas, which makes the situation more vulnerable and causes stress on infrastructure, heightened competition for resources, and contributes to global climate alterations which impact burden on the world's infrastructure and human population (UNDESA, 2018; IPCC Cities, 2022). According to WPP 2022, South and Southeast Asia is the most populous region. So, we selected two deltaic megacities of South and Southeast Asia namely the Bangkok Metropolitan Region (BMR) and the Kolkata Metropolitan Region (KMR). KMR is one of India's biggest urban agglomerations, positioned at the Ganga River delta, at an average altitude is about 8 m above mean sea level, with a population of 14.72 million people roughly 7950 people per square kilometer as per the 2011 Census report with an annual population growth rate of 1.8% in between 2001-2011, expecting an increase of 20 million by 2021 and 21.1 million by 2025 (Malik et al., 2020, Maity et al., 2022). The normal annual rainfall that had been recorded was 1647 mm. The mean temperature is recorded at 22.50 °C in the months of winter which goes down 10 °C in December to January. The mean temperature is recorded at 29.25 °C in the months of summer which goes up to 40 °C in April (Hasnine et al., 2023). On the other hand, BMR covers an area of approximately 6113.30 km2, with a population of nearly 10 million (as of 2019) roughly 1400 people per square kilometer, located on the Chao Phraya River basin's flat terrain, ranging at 4m above sea level (SFD Bangkok, 2020). The BMR experiences three seasons: summer (March), monsoon (June–October), and winter (November–February). (T.Taichi 2020) with an average precipitation of about 1700 mm/year. The mean temperature is recorded at 35°C - 40°C in the months of summer in April and a minimum of 16°C - 25° in January (Pakarnseree et al., 2018).

The accelerated urbanization and industrialization arising in metro cities are converting wetlands, agricultural lands, and vegetation into built-up areas, resulting in detrimental effects on water security, and biodiversity, the emergence of urban heat islands, and alterations to the microclimate (Filho et al. 2021). Asia and Africa are expected to experience the greatest loss of green areas by 2030 (d'Armour et al., 2017). From 1990 to 2020, around 420 million hectares of forest land were destroyed to meet demand, with 90% of this destruction occurring in tropical areas, which poses a threat to the environment, considering that approximately 45% of the total forest land is in the tropics (IPCC Tropical Forest, 2022). A decrease in the green land or open space correlates with an increase in concrete area and an increase in vehicular services (d'Armour et al., 2017).

In metropolitan areas construction and developments involve activities that generate dust, harmful emissions from construction sites, and particulate matter which are responsible for worsening the air quality, thus leading to air pollution. Besides construction and development sites affecting air quality, industrial expansion, higher vehicle density, and traffic congestion in urban areas are also responsible for producing volatile organic compounds, sulfur dioxide, and harmful gases that threaten human life. Studies suggest that 23%-50% of these emissions come from transportation in developing countries (Crippa et al., 2018). So, air pollution is a major concern in recent decades. It not only alters the local climate but also affects human health. According to the reports of UN-Habitant 2022, air pollution is responsible for about 7 million premature deaths annually. The concentration of air pollutants such as tropospheric ozone, oxides of nitrogen, and volatile organic compounds are likely to peak in the mid-centuries due to urban sprawl in Southeast Asia, South Asia, and Africa (Naik et al., 2021). In 2023, Thailand's PM2.5 concentration surged by 28% from 18.1 µg/m3 to 23.3 µg/m3, with Bangkok recording an annual average of 21.7 µg/m3 and only one district, Samut Prakhan, staying below the WHO recommended level, while cities like Chiang Mai surpassed it by 150%; India, ranking third for poor air quality, saw concentrations rise from 53.3 µg/m3 to 54.4 µg/m3 between 2022 and 2023, with Delhi witnessing a 10% increase to a monthly average of 255 µg/m3 in November, and countries in South and Central Asia recorded the highest annual average PM2.5 concentrations in 2023(World Air Quality Report, 2023). The consequences of urbanization are not limited to air pollution and scarcity of land but also affect the global climate. As well as concrete structures and high-rise structures have higher heat absorption and emission capabilities, making urban areas warmer than rural areas (Chakraborty et al., 2021a).

Increase in global average temperature and heat waves are the outbreaks of climate change and will impact the urban system (Doblas-Reyes et al., 2021). July 2023 is marked as the warmest month as well as the warmest year with a rise of 1.45^{o}C (+/- 0.12 ^{o}C) in global mean surface temperature after the 1850-1900 mark, historically placing it among the nine warmest years on record from 2015-2023, previously 2016 with an anomaly of 1.29^{o}C (+/- 0.12^{o}C) and 2020 with an anomaly 1.27^{o}C (+/- 0.13^{o}C) recorded as the warmest year in the decade (WMO, 2023). The ultimate cause of the increase in global temperature is the increase in the atmospheric concentrations of greenhouse gases where countries like India, Thailand, Myanmar, Malaysia, and Vietnam are located in the South and Southeastern parts of Asia and are thereby highly influenced by large-scale seasonal reversal wind regimes called monsoon (Serreze and Barry, 2010). Though monsoonal rainfall and temperature are inversely correlated, the consequences of temperature changes over the past few years resulted in alterations in global monsoonal precipitation reduced by approximately 70%, its implications not only for the Indian summer monsoon but also for Southeast Asia, where it delays the arrival of the monsoon by 15 days (Ashfaq et al., 2009). Due to heavy rainfall, urban areas are vulnerable to floods or waterlogging. The capital of West Bengal, Kolkata encountered an unprecedented 236mm of rainfall in a single day on May 20, 2020, after the downfall of the heavy cyclone, which boosted the city’s total rainfall of 359.1mm only in May in contrast to the average May rainfall of 117.5mm in between 2010-2019 which caused waterlogged in the major parts of the city (Mukherjee et al., 2021). In July 2017, Kolkata witnessed severe flooding from heavy rainfall of 621.5mm, leading to the awful demise of approximately 50 lives, and the evictions of 2 million people across 160 villages that remained underwater for days (The Hindu, 2017). Kolkata conditions akin to flooding due to its soil composition which shows tremendous capacity for runoff and offers a low infiltration rate due to its silty and loamy nature the remaining part of Kolkata shows a clayey soil with very low porosity leads to excessive surface runoff, and the landform of Kolkata is characterized by its extremely gradual slope and saucer-like structure similar to the active delta region, automatically worsening with excessive runoff after one or two hours of heavy rainfall (Bose et al., 2023). Besides Kolkata, Bangkok's rapid population, improper drainage system, upstream changes in northern Thailand, tidal effects, and land subsidence from ground extraction have led to flash floods in Bangkok city (Marks et al., 2020). Bangkok's improper drainage system is due to the ground surface level being lower than the controlled water level in the surrounding canal and the Chao Phraya River which reduces the efficacy of gravitational drainage and enhances flash floods in the city (Urbanisation of Bangkok., 2022). Bangkok goes through a tropical savanna-type climate, with distinctive rainy and dry seasons, it experiences about 1651mm of rainfall annually, and almost all precipitation occurs between May and October, or the rainy seasons (T.Taichi 2020). Considering the above, this study addresses the urban vulnerability of the deltaic megacities regarding social and physical evaluation from the unscientific growth of urbanization and increasing demand for natural resources.

1.1 Aim

The aim of this study is the assessment of the vulnerability zones in the Metropolitan Region of the Hooghly River Delta, Kolkata, India, and the Chao Phraya River Delta, Bangkok, Thailand.

1.2 Objectives

The objectives of this research are:

i. To evaluate the distribution of nine parameters (i. Rainfall, ii. LST, iii. AQI, iv. NDBI, v. NDVI, vi. Population Density, vii. Old/Child Population, viii. Per Capita Income, ix. Literacy Rate)

ii. To access the spatial zones of vulnerability and prepare map

Chapter 2: Literature Review

2 Literature Review

Urban Vulnerability has become a headache in growing metropolises which increases the risk of both natural and anthropogenic activities. The urban areas face immense environmental, socio-economic, institutional, and infrastructural struggles. This literature review revolves around the recent study on urban vulnerability and its risk index by prioritizing the parameters directly involved in shaping the vulnerability.

2.1 Rainfall:

Rainfall has a pivotal impact on the context of urban vulnerability. Insufficient rainfall may lead to drought, water scarcity, and an increase in temperature, and on the other hand, heavy rainfall can contribute to urban flooding, landslides, damage to the infrastructures, and increased water-borne diseases. Thus, Bose et al., 2023, analyze the consequences of two consecutive hours of heavy rainfall at various rainfall depts on flooding in Kolkata, India employing the Integrated Valuation of Ecosystem Services and Trade-Offs-Urban Flood Risk Mitigation (InVEST-UFRM) model. The investigation shows that approx. 75% of the surface area is impermeable, which boosts the flood risk and causes runoff, especially in the northern part of the city. As many metropolitans do have not proper drainage infrastructure, studied by Chitwatkulsiri et al., 2021 in the Sukhumvit area, Bangkok, they developed a system that includes rainfall run-off modeling, flood inundation mapping and collection of rainfall forecast data and the outcomes accurately estimated flood zones and water levels within an hour of rainfall data and allowing for early warnings enables effective flood management methods such as pumping, watergate controls, and evacuations are made possible by this process. Heavy rainfall not only causes flash floods but also destructs the hydrological structures, Guhathakurta et al., 2011 analyzed the frequency of rainy days, rain days, heavy rainfall in a single day, monthly average rainfall of the monsoon period and return period at various locations of India to observe the rainfall pattern as well as the consequences of climate change on heavy rainfall and risk of flood intensity of the area. The result concluded that the peninsula, eastern part, and northeast of India have the highest frequency of extreme rainfall rather than the central part. In addition, Patil et al., 2023, also advised that the hydrological planning of India needs to take into account the current extreme rainfall patterns to ensure the bearing capability of the infrastructure during heavy rainfall and also suggested finding natural restoration processes such as conservation of wetlands, strengthening watershed management to ensure safety. Alike, Roxy et al., 2017, added as the frequency of extreme rainfall increases in the parts of India due to climate alterations which exhibit flash flood risk of the area as its infrastructure may not have designed to handle such events.

2.2 Air Quality Index (AQI):

AQI is a key indicator to assess the concentration of air pollution as well as its impacts on human health in association with urban vulnerability. Thus, Zhang et al.,2016, offer an approach to vulnerability assessment of the environment due to anthropogenic interference by implementing GIS, MCDA, and Ordered Weighted Averaging (OWA) techniques in the Exposure-Sensitivity-Adaptive Capacity (ESA) framework at the Beijing-Tianjin-Hebei region of China, his results affirm the reliability and shed light on the urgent action for air pollution needs to be addressed and also offers ideas for methodical decision-making and future acts for the policymakers. In 2018, again Zhang et al. established a Comprehensive Air Quality Model with the Extensions (CAMx) method for the atmospheric vulnerability assessment in the same study area focusing on the parameters including socio-economic factors, atmospheric factors, and anthropogenic activities. This method was proven to reduce atmospheric vulnerability and can be a useful tool for guiding policymakers and results indicate the central region and the southern region are at higher risk zones due presence of higher AQI. Equivalently, Maji et al., 2017, explored the impacts of air pollution on human health in various locations of Indian cities, and shed light on the concentration of particulate matter PM2.5 and PM10 and its association with higher mortality rates and increasing cardiovascular diseases in human health. This study also stresses the increased urban vulnerability among the old/child population and heightened the risk of asthma. Furthermore, Nishad et al., 2015 added the amount of NO_X and SO_X generated by vehicular actions can also severely impact human health and the environment. Similarly, Gurjar et al., show an in-depth assessment of issues related to air pollution in Indian megacities such as Kolkata, Mumbai, Delhi, and Chennai providing stresses on the trends in emission and air quality enhancement initiatives from the government to minimize air pollution in urban areas, it emphasizes the importance of addressing vehicular emissions and also determines the trends in concentration and pollutant emission over the megacities. Moreover, Sun et al., 2024, compared air pollution with urban green space and suggested how open green space reduces the concentration of air pollution also the study highlighted the importance of urban planning in the reduction of AQI in well-developed metropolitans.

2.3 Land Surface Temperature (LST)

LST is an integral indicator of understanding and assessing urban vulnerability. Hung et al., 2022, revealed in his study in China that an increase in LST leads to atmospheric dryness resulting in vegetation loss and drying of the urban areas this phenomenon is termed Urban Heat Island (UHI). So, Zhou et al., 2011 studied the comprehensive trends of LST. It correlated them with urban sprawl using satellite images from Landsat and Modis and concluded that the primary causes of increasing LST and generating Urban Heat Island (UHI) in the metropolis are the lack of green space which gets sacrificed due to industrial development, unorganized or dense settlements, and rapid population growth. Similarly, Vargas et al., 2020, in their study in Mexico, showed how $3^{O}C$ - $4\ ^{O}C$ of temperature has increased in the study area in the last decades and Zhou et al., 2016 explain that an increase in LST not only sacrifices vegetation but also triggers the frequency of intense storms, natural hazards related to the warm spell, and increases risk to urban flooding. In addition, Mirzeai et al., 2020, showed other impacts of LST on the environment, it exhibits the frequency of health disputes in humans.

2.4 Population Density:

Urbanization in cities is a challenging issue fuelled by a range of environmental, socio-economical, and infrastructural concerns. Population density is said to be the backbone of social urban vulnerability. So, Liu et al., 2016, proposed that population density triggers the chances of environmental vulnerability such as heatwaves, air pollution, and urban flooding. Urban areas lack green spaces due to unorganized and dense settlements and have high levels of impermeable surfaces which boost the heat island effect and reduce natural water infiltration which leads to scarcity of fresh drinking water and triggers natural hazards. Cutter et al., 2015, mentioned that social vulnerability and population density are interrelated, the higher the population density the more is the huge stress on natural resources, these factors trigger the vulnerability of human health and they lack the adaptive capacity to respond. Most of the urban areas are unplanned and are much more susceptible to natural hazards. So, Rezaei et al., 2023, analysed three fundamental criteria such as physical vulnerability, adaptive capacity, and emergency response accessed in a seismic vulnerability by evaluating 19 districts of Iran employing the Analytic Hierarchy Process (AHP) and concluded that lack of open space, limited emergency services, high population density are contributors of urban vulnerability. Similarly, Solecki et al., 2015, showed in their studies how New York’s higher population density leads to storm surges and rise in sea level has increased vulnerability. According to the UN’s city prospects 2022 report, Mumbai is one of the urbanized areas of India that faces challenges due to urbanization and dense population from heavy rainfall and infrastructural issues

Chapter 3: Study Area

3 Study Area

3.1 Physiography of Study Areas

Kolkata Metropolitan Area (KMA) is located in the lower deltaic region of the Ganga-Brahmaputra-Meghan delta with an altitude of approximately 6m above sea level. It is recognized as the third largest metropolitan in India and the largest urban area in the eastern part with a population of about 14.72 million and a population density of 7950 people per sq. km, as per the 2011 Census report. It comprises an area of 1886.67 sq. km and stretches between 22° 21' 36" N to 23° 4' 48" N latitude to 88° 23' 24" E to 88° 25' 12" E longitude. The Hooghly River passes through the of the study area and connects with the Bay of Bengal. Its major districts are Howrah, Hooghly, Nadia, North 24 Parganas, and South 24 Parganas. This city experiences tropical wet and dry climate throughout the year. The maximum temperature rises during the summer months of May and June up to 32º C - 42º C and the minimum temperature falls during the winter months of December - January up to 10º C - 26ºC on average. From June to September, the average rainfall in KMA is approximately 1158-1650 mm. The gradual conversion of extensive agricultural plains into densely populated urban areas and a noticeable rise in population over the years have dramatically hastened the economic expansion of the Kolkata Metropolitan Area (KMA). Hence, KMA is said to be a suitable study area for the assessment of urban vulnerability (Census of India, 2011).

Bangkok Metropolitan Region (BMR) is situated on the lower deltaic plain of the Chao Phraya River, which flows through the centre of the city and surrenders to the Gulf of Thailand in the south with an altitude of about 4m above sea level. BMR is considered the largest urban area in Thailand with a population of 10.8 million and a population density of about 5293.3 people per sq. km. It extends over 7761.6 sq. km. and stretches between 13°42′30″–13°47′42″N latitudes and 100°25′27″–100°32′58″E longitude. BMR comprises 6 provinces: Bangkok, Nakhon Pathom, Pathum Thani, Nonthaburi, Samut Prakan, and Samut Sakhon. The city offers a tropical wet and dry climate throughout the year so, it experiences three seasons: summer (March-May), monsoon (June – Oct), and winter (Nov – Feb). The summer months of March-May are considered the warmest months experiencing about 35ºC - 40ºC. During winter it experiences about 18º C - 20º C on average and annually receives 1,188 – 1,510 mm of precipitation. Therefore, BMR is facing heightened stress due to the population's unscientific growth, affecting the country's economic expansion. Hence, BMR is said to be a suitable study area for the assessment of urban vulnerability (Thailand Metrological Department).

Table 1. Details of study areas

Location	**Average Temperature (ºC)**	**Average Rainfall (mm)**	**Type of Climate**	**Average AQI**	**Average Altitude**	**Population Density**
KMA	26.8	1650	Tropical wet and dry climate	101.14	6	7950
BMR	30	1510	Tropical wet and dry climate	88.03	4	5294

Source: Indian Metrological Department and Thailand Metrological Department

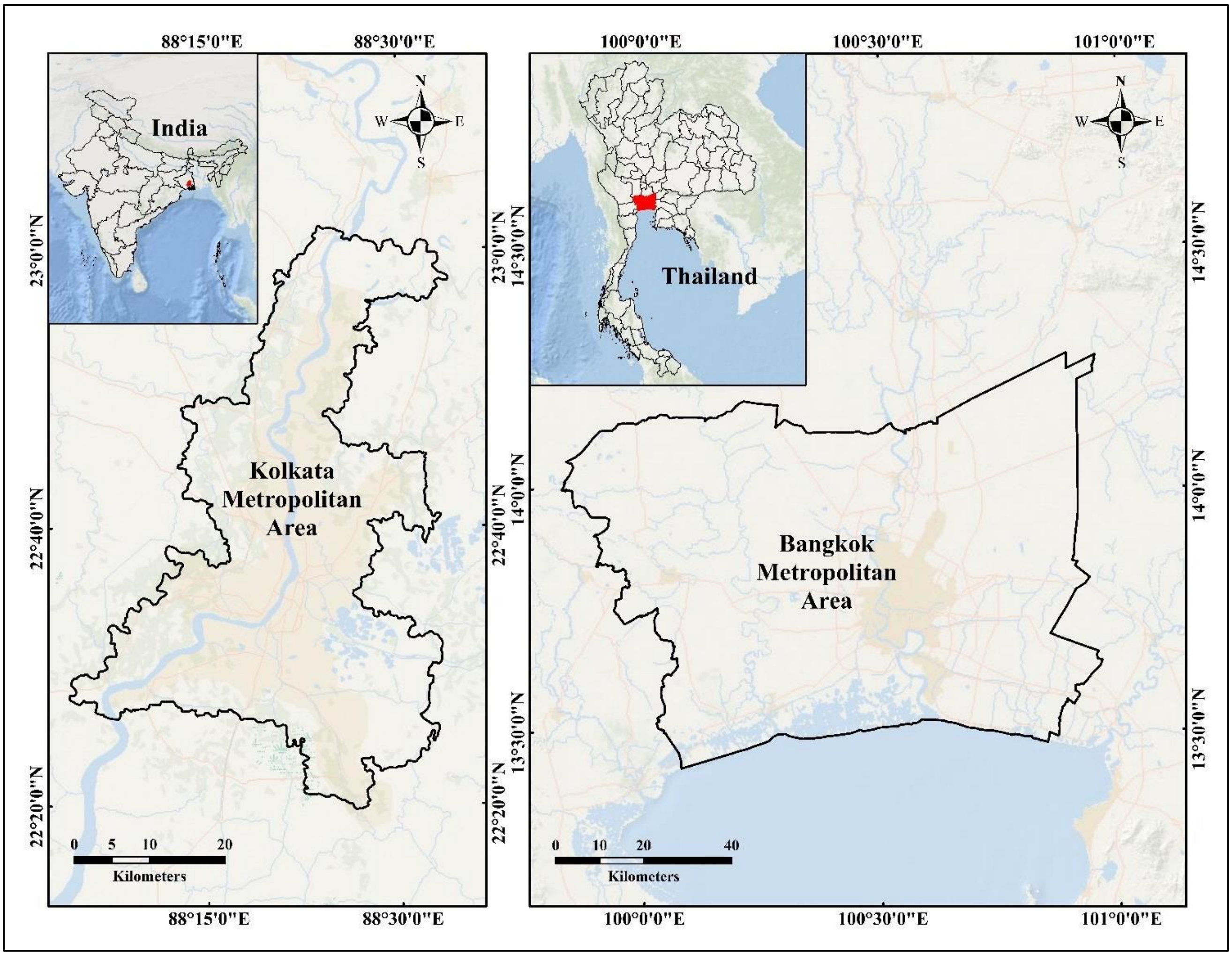

Figure 1. Geographical representation of Study Area

Chapter 4: Materials and Method

4 Materials and Method

4.1 Data acquisition and preparation techniques

To access the Urban Vulnerability Index (UVI) of KMR and BMR, this study used extensive non-spatial attribute data and spatial data from various sources. Based on previous literature, this study selects nine indicators based on hazards, exposure, and vulnerability including population density, literacy rate, per capita income, rainfall, Land Surface Temperature (LST), Air Quality Index (AQI), NDVI, and NDBI was used to evaluate the Urban Vulnerability of the study area.

Table 2. Selected indicators of the UVI model and their sources

Sl. No.	**Parameters**	**Data Types**	**Source**	**Resolution**
Kolkata Metropolitan Area				
1	Rainfall	.csv	Meteorological Department of India	-
2	AQI	.csv	CMAQ	-
3	LST	Landsat 8	USGS	30 m
4	NDBI	Landsat 8	USGS	30 m
5	NDVI	Landsat 8	USGS	30 m
6	Population Density	.csv	Census of India	-
7	Old/Child Population	.csv	Census of India	-
8	Per Capita Income	.csv	Census of India	-
9	Literacy rate	.csv	Census of India	-

Table 2. Continue…				
Sl. No.	**Parameters**	**Data Types**	**Source**	**Resolution**
Bangkok Metropolitan Region				
1	Rainfall	.csv	Thailand Meteorological Department	-
2	AQI	.csv	CMAQ	-
3	LST	Landsat 8	USGS	30 m
4	NDBI	Landsat 8	USGS	30 m
5	NDVI	Landsat 8	USGS	30 m
6	Population Density	.csv	National Statistical Office, Thailand	-
7	Old/Child Population	.csv	National Statistical Office, Thailand	-
8	Per Capita Income	.csv	National Statistical Office, Thailand	-
9	Literacy rate	.csv	National Statistical Office, Thailand	-

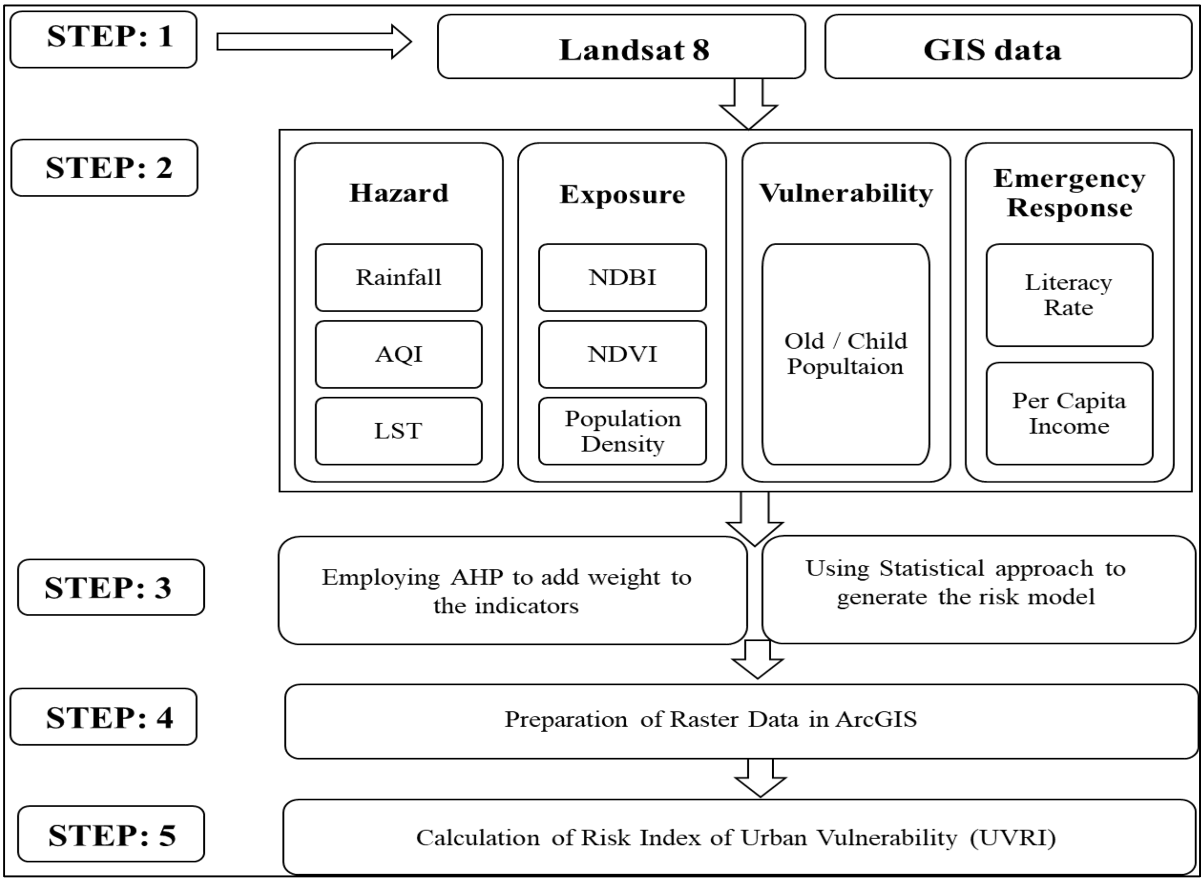

Figure 2. Step by step procedure to evaluate Urban Vulnerability

4.2 Parameter Introduction

4.2.1 *Rainfall:*

The primary driver of urban vulnerability is rainfall, and continuous heavy rain can cause a threat of waterlogging in urban areas (Peng et al., 2014). The intensity of rainfall plays a crucial role not only in climate change but also in crop production and agriculture.The various rainfall data were collected for the years 1991, 2001, 2011, and 2021 from the India Meteorological Department (IMD). The study areas receive monsoon from June to September.

4.2.2 *Air Quality Index (AQI):*

This study applied the Fused Air Quality Surfaces Using the Downscaling (FAQSUD) mechanism suggested by the US Environmental Protection Agency (EPA) and the Community Multiscale Air Quality (CMAQ) to collect relevant air quality data, for accurate projections of air toxics, ozone, particulate matter, and acid deposition are obtained by the CMAQ model, known as EPA's primary source for tracking air quality at region and global level. It incorporates air quality modeling with the current developments in meteorological research and high-performance computing. For the area of concern, we utilized downscaled daily forecast data that included monthly mean concentrations of PM2.5 and PM10.

4.2.3 *Land Surface Temperature (LST):*

LST indicates the skin temperature of the ground surface, determined by satellite thermal data, which impacts the energy transfer between the ground surface and vegetation and influences air temperature. This study employs a split window algorithm method based on TIRS band, found in between 10 – 12 µm on the atmospheric window suggested by McMillian in 1975. The method is as follow:

$$T_s = T_i + c_1 (T_i - T_j) + c_1 (T_i - T_j)^2 + c_0 + (c_3 + c_4 w)(1 - \mathcal{E}) + (c_5 + c_6 w) \Delta_{\varepsilon}$$

Equation 1

where, T_i *and* T_j denote the brightness temperatures of bands i and j, whereas $\mathcal{E}$ illustrates land surface emissivity, derived as $\mathcal{E} = 0.5 (\mathcal{E}_i + \mathcal{E}_j)$; on the other hand, Δ_{ε} represents the deviation in emissivity stated as $\Delta_{\varepsilon} = (\mathcal{E}_i + \mathcal{E}_j)$; w assessed as total atmospheric water vapors content in 1 gm/cm; and c_0 - c_6 represents the split window coefficient values utilized in this method.

Table 3. Temperature of the study area throughout the year

Study Area	Summer	Monsoon	Winter
BMR	mid-February to mid-May	mid-May to mid-October	mid-October to mid-February
Temperature	30°C – 40°C	26°C – 34°C	18°C – 22°C
KMA	March – June	July – October	November - February
Temperature	30°C – 42°C	26°C – 36°C	18°C – 21°C

Source: Indian Metrological Department and Thailand Metrological Department

4.2.4 *Normalized Difference Built-up Index (NDBI):*

NDBI is a critical measure of heat wave sensitivity as it accounts for the spatial expansion of buildings, the growth of built-up areas, and the density of urban areas all of these increase sensitivity (Gabriel et al., 2011). Gather multispectral Landsat 8 imagery of the specified area, including the bands needed for calculating the NDBI. To calculate NDBI the formula would be:

$$NDBI = \frac{SWIR - NIR}{SWIR + NIR}$$

Equation 2

where, SWIR stands for the reflectance in the short infrared band (Band 7 or Band 6) and NIR represents the reflectance in the near-infrared band (Band 5).

4.2.5 *Normalized Difference Vegetation Index (NDVI):*

NDVI is widely used remote sensing tool to assess the vegetation cover on Earth's surface (Chen & Brutsaert, 1998; Gillies et al., 1997; Weng & Lo, 2001). The NDVI scale runs from -1 to +1, a value close to or near 0 represents areas with less vegetation, especially urban areas and wasteland, -1 represents waterbodies whereas +1 denotes very healthy vegetation and dense forest. This study employed NDVI to explore the relationship between Earth's surface temperature and live green vegetation. The calculation include:

$$NDVI = \frac{NIR - Red}{NIR + Red}$$

Equation 3

Where, Red represents TM band 3 and NIR represents the reflectance in the near-infrared band 4, vegetation reflects.

4.2.6 *Population Density:*

Unscientific growth in population density results in urbanization, water shortage, and greater susceptibility to natural disasters and also poses threats to poor human health, poverty, and a low standard of living (Groce et al., 2009). The data of KMR are collected from the Census of India and Data of BMR are collected from the National Statistical Office, Thailand.

4.2.7 *Old/Child Population:*

Unscientific population growth largely affects the most vulnerable groups such as infants, old age, and female population. In a metropolis overstressed population, pollution, scarcity of fresh water, malnutrition, and diseases due to improper livelihood are common. So, Gracy M, 2000, suggested the urgent requirement for proper management and organized policymakers to mitigate such challenges. Additionally, a study by Lelieveld et al., 2015, showed how an improper environment leads to public health threats and causes 381,000 premature deaths annually only in Europe and also contributes to biological risks to adolescents which has a long-term effect. United Nations, 2015, finds that older populations are less susceptible in urban areas due to improper healthcare, social isolation, and mobility issues. The percentage of Old/Child Population in the years 1991, 2001, 2011, and 2021 has been collected from the Census of India data and the National Statistics of Thailand.

4.2.8 *Per Capita Income:*

Economic ability increases the adaptive capacity of the person in the context of facing any vulnerable disaster. Generally, studies suggested that high-income groups are much more susceptible to urban vulnerability as compared to low-income group (Duan et al., 2022). The Per Capita Income of household in the years 1991, 2001, 2011, and 2021 has been collected from the Census of India data and the National Statistics of Thailand.

4.2.9 *Literacy Rate (LR):*

Knowledgeable people are much more aware of the consequences of the ongoing hazards such as heatwaves, and urbanization as compared to illiterate people (Hess et al., 2012). The rate of literacy in the years 1991, 2001, 2011, and 2021 has been collected from the Census of India data and the National Statistics of Thailand.

4.3 Urban Vulnerability Index Modeling

4.3.1 *Analytic Hierarchy Process (AHP)*

The Analytic Hierarchy Process (AHP) is considered a highly adaptable decision-making technique that mirrors natural human thought processes and behaviors. This technique evaluates complex problems by analyzing their interrelated effects, simplifies them into a more manageable form, and provides solutions. AHP is applicable when dealing with decisions involving multiple choices or criteria, particularly when they are competing. The criteria can be considered quantitatively and qualitatively. This decision-making method relies on underlying paired comparisons with table 4. The decision-maker starts by creating a hierarchical structure. The hierarchical decision tree displays the comparable factors and assesses the competing alternatives. Subsequently, a series of paired comparisons are conducted. The comparisons reveal the weight of each factor relative to the competing alternatives in the decision-making process. Finally, the Analytic Hierarchy Process (AHP) integrates the pairwise comparison matrices to facilitate a more informed decision.

The principles of AHP, as defined by Saaty (2008), follow these steps:

i. Identify the problem and specify the type of information needed

ii. Organize the decision hierarchy starting with the overall goal at the top, followed by broad objectives, intermediate levels (criteria that influence subsequent elements), and ending with the lowest level, which typically consists of the alternatives, as shown in Table 4.

iii. Create a series of pairwise comparison matrices for consistency check, as shown in Table 5. Each element at a higher level is used to compare the elements in the level directly below it concerning that higher-level element

iv. Apply the priorities derived from the comparisons to assign weights to the priorities in the level directly below. Repeat this for each element. Then, for each element at the lower level, sum its weighted values to determine its overall or global priority. Continue this process of weighting and summing until the final priorities of the alternatives at the bottom level are determined

Table 4. Relative importance scale (1-9)

The intensity of importance of the indicators	Numeric Value
Equal importance	1
Moderate importance	3
Strong importance	5
Very strong importance	7
Extreme importance	9
The median value of two adjacent judgments	2, 4, 6, 8

Table 5. Random Consistency Index (RI) check table

No. of criteria (n)	1	2	3	4	5	6	7	8	9	10
RI	0	0	0.58	0.90	1.12	1.24	1.32	1.41	1.45	1.51

The whole AHP process is categorized into five steps: (i) creating a hierarchical structure model; (ii) developing a judgment matrix; (iii) hierarchical single ranking; (iv) verifying the consistency of the judgment matrix; and (v) hierarchical total sorting. The weight calculation results for each index are presented in Table. 6.

Table 6. Weight of indicators

Target Layer	Criteria layer	Criteria layer weight	Indicator layer	Normalized weight (Winter)	Normalized weight (Summer)	Normalized weight (Monsoon)
Urban Vulnerability Index (UVI)	Hazard	0.42	Rainfall	0.11	0.13	0.63
			AQI	0.66	0.31	0.12
			LST	0.23	0.56	0.25
	Exposure	0.11	NDBI	0.36	0.49	0.47
			NDVI	0.31	0.23	0.19
			Population Density	0.33	0.28	0.34
	Vulnerability	0.16	Old/Child Population	1	1	1
	Emergency Response	0.23	Literacy Rate	0.52	0.52	0.52
			Per Capita Income	0.48	0.48	0.48

4.4 Urban Vulnerability Index Modeling Criterion Layer

A population's susceptibility to environmental threats is evaluated by its extent of exposure, sensitivity, and adaptability. The four criteria layers were constructed based on four parts of natural disaster risk formations including hazard, exposure, vulnerability, and emergency responses with recovery capabilities. The number of natural variations impacts the risk assessments of UVI such as the greater the risk, the higher the possibility of disaster. The criteria layers are:

The Hazard (*H*) represents the possibilities of occurrence of urban vulnerability disasters, the lower value of H reflects the lesser chances of occurrences of urban vulnerability. This study considers Rainfall, AQI, and LST as hazard.

The Exposure (*E*) indicates the threats of risk to all the properties and people from the urban vulnerability, essentially the higher the density of the people and properties enhances the probability of losses through urban vulnerability. Similarly, this study considers NDBI, NDVI, and Population Density as exposure.

The Vulnerability (*V*) quantifies the extent of losses faced by individuals and properties in dangerous areas due to urban vulnerability and measures its capacity to sustain such emergencies. The greater vulnerability corresponds to greater disaster losses and higher risk. This study considers the most vulnerable group to be the Old/Child population.

The Emergency response and its recovery capacity (*C*) is referred to as the capacity to react and rebound from calamities that occur due to urban vulnerability effectively while incorporating disaster-resistant material reserves, emergency management skills, and investment in disaster prevention and accessibility to its associated resources. This study considers Literacy Rate and Per Capita Income as the emergency response categories for vulnerability.

4.5 Urban Vulnerability Risk Index Modeling:

In this study, the Urban Vulnerability Risk Index (UVRI) revealed a positive interrelation between hazard, exposure, and vulnerability, and a negative interrelation with emergency response and its recovery capacity. The formula will be:

$$UVRI = \frac{H \text{ x } V \text{ x } E}{1 + C}$$

Equation 4

Table 7. Scale on the basis on Urban Vulnerability (0-10)

The intensity of Urban Vulnerability	Numeric Value
Low	0 – 5
Low - Moderate	5 – 6
Moderate	6 – 7
Moderate- High	7 – 8
Very - High	8 - 10

Based on the numerical value presented in the table, we can conclude the intensity and the probability of the occurrence of Urban Vulnerability in the study area. The range (0 – 5) is categorized as a less vulnerable zone. Similarly, the range (5 – 6) interprets low to moderate vulnerable zone. Additionally, the range (6 – 7) indicates a moderate vulnerable zone, and the range (7 – 8) indicates a moderate to high vulnerable zone. Lastly, the range (8 – 10) shows the highest vulnerable zone.

Chapter 5: Results and Discussion

5.1 Results

All demographical, socio-economic, metrological parameters noted here are appear to have an association with the Urban Vulnerability Risk Index (UVRI).

5.1.1 *Hazard (H)*

5.1.1.1 Rainfall:

Figure 4a displays the rainfall of BMR during winter which shows that the upper region especially the northern, northeastern, and northwestern regions of Nonthaburi-Nakhon Pathom-Pathum Thani about 60% of the area experienced very little rainfall of about <50mm, and the remaining areas of the central region Bangkok Metropolis, Samut Prakan in the southeastern area and Samut Sakhon in the southwestern part about 40% approximately of the area gets rainfall of about 50-100mm. Figure 4b, displays the BMR during monsoon which varies between moderate to high. The central part of Bangkok Metropolis, Samut Prakan in the southeastern area, and areas of Samut Sakhon in the southwestern part of about 58.18% approximately of the area received high rainfall of about 150-200mm and the areas about 41.8% of the area of Nakhon Pathom in the northwestern region, Samut Sakhon in the southwestern region, Nonthaburi on the northeastern region, and Pathum Thani in the northern region experienced a moderate rainfall of about 100-150mm. During summer, figure 4c illustrates that about 47.71% approximately of the area of the southern part of Samut Prakan, the central region of Bangkok Metropolis and the northern region Pathum Thani receives moderate rainfall of about 100-150mm. Lastly, about 52.29% approximately the remaining areas of the western part receive less rainfall of about 50-100mm.

Figure 4d, portrays the rainfall of KMA during winter which shows that about 33.64% of the region in the western part of Hooghly-CMC and Kalyani in the northern region experience very low rainfall of about <50mm. The remaining region of about 66.36% of the area observed moderate rainfall of 100-150mm. Figure 4e presents, the average rainfall of the KMA during monsoon, the major areas of about 78.18% of the area including the central part of KMC, the southern region South 24 Parganas-Maheshtala-Budge Budge, and the northeastern part North 24 Parganas-BMC-Kamarhati, and the southeastern part experienced heavy rainfall of >200mm, which was stated as a very highly vulnerable condition during monsoons and increased the probability of urban flood and the western areas Hooghly-CMC and its surroundings and the northern areas of about 21.82% of the area received a highly average rainfall of about 150-200 mm. Figure 4f, portrays the average rainfall of the KMA during summer, about 58.66% of the regions of the eastern part and northeastern part North 24 Parganas-Kamarhati-BMC and the southern part of the KMA received moderate rainfall of about 100-150 mm, and the western, southwestern, and northwestern Hooghly-CMC-Howrah and the northern region Kalyani about 41.34% of the area experienced low rainfall of about 50-100mm.

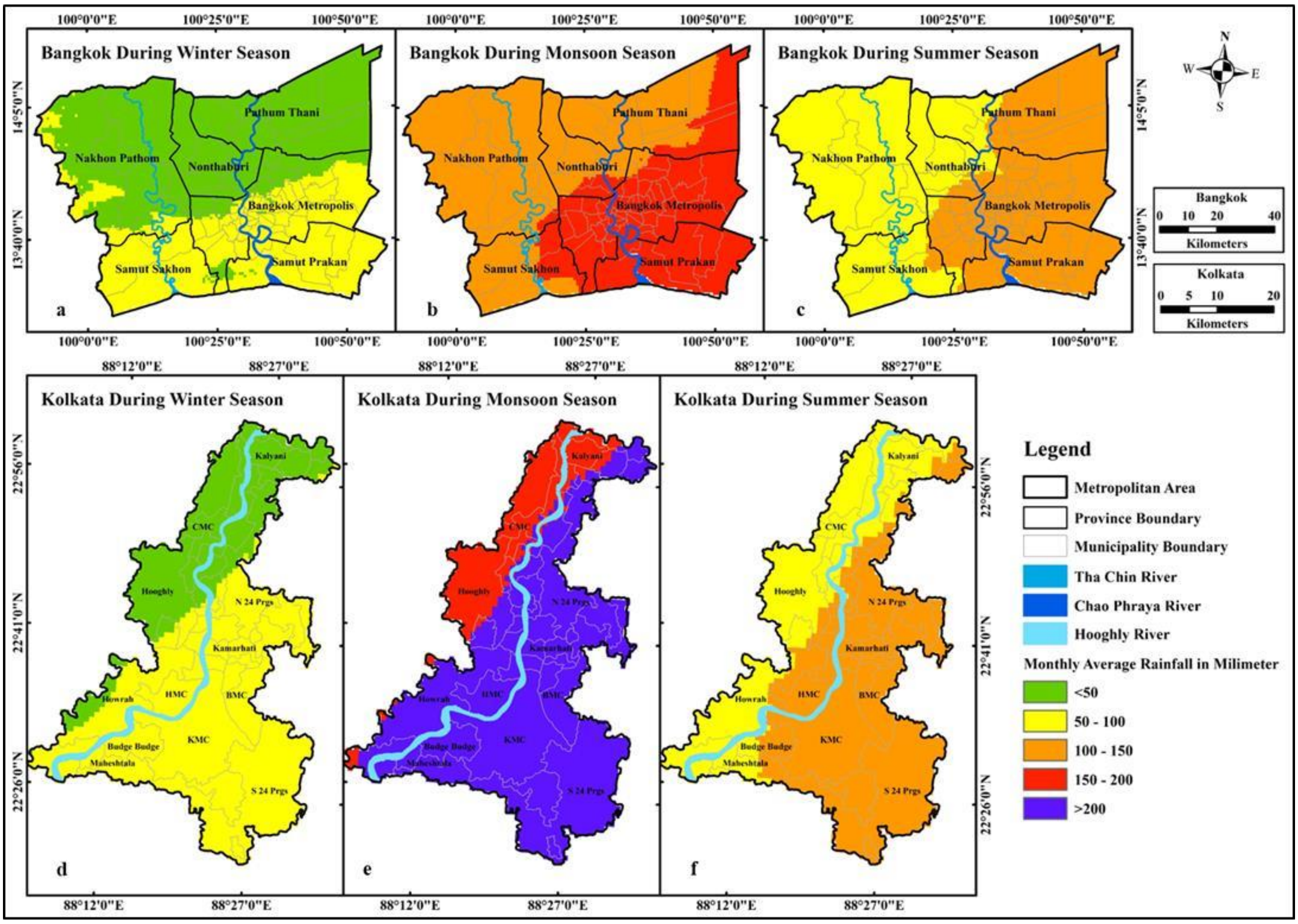

Figure 3. Monthly Average Rainfall (mm) of BMR and KMA in each season

5.1.1.2 AQI:

For BMR, Figure 5a shows that in winter, the AQI falls into the range of 150-200 of about 22.57% area in the central region of Bangkok Metropolis and western Nakhon Pathom areas, which are said to be high. The rest of the area of about 69.42% has a moderate AQI range of 100-150 and a few areas of about 8.01% have a low AQI of 50-100. As shown in Figure 5b, about 69.43% of BMR has a healthy AQI below 50 in the monsoon. This is a big improvement compared to other seasons. The northern region Pathum Thani and western Nakhon Pathom of about 30.57% of the area have a low AQI of 50-100. In summer, figure 5c portrays AQI levels over BMR range from less to moderate vulnerability. The central Bangkok Metropolis, together with Pathum Thani in the north and Nakhon Pathom in the west of about 22.45% area, shows an AQI range of 100-150, a moderate range and few areas of about 2.45% shows an AQI below 50 and the remaining areas of about 75% show an AQI of 50-100.

In winter, both KMA and BMR suffer from their poorest AQI. Figure 5d depicts that in winter season, most areas in KMA fall under the "inferior" to "poor" AQI range. More than 200 AQI, characterizing them as extremely high, it is in areas covering about 12% of the central and southern parts. Specifically, the northern, western, and eastern zones—including districts of Kalyani – Howrah - North 24 Parganas of about 71% have AQI ranges of 150 to 200, showing highly poor AQI. Others are found to be moderately vulnerable of about 17%, where the AQI varies from 100 to 150. In contrast, in Figure 5e, the monsoon season reveals a generally improved situation regarding AQI over KMA. Of the total area, around 69% of the area comprised an AQI below 50, mainly towards the centre (KMC), southern, and parts of the northern regions of about 25%, which observe an AQI of 50-100 and rest areas of about 1% have an AQI of 100-15, moderately vulnerable range. Figure 5f, shows in summer, the AQI range returns to a moderate range where about 75% of the area witnesses an AQI of 100-150. The western and eastern parts, covering Hooghly and North 24 Parganas, of about 23% area fall in the range of an AQI level of 50-100, while in the central KMC area of about 2% area, the AQI is recorded in the range of 150-200.

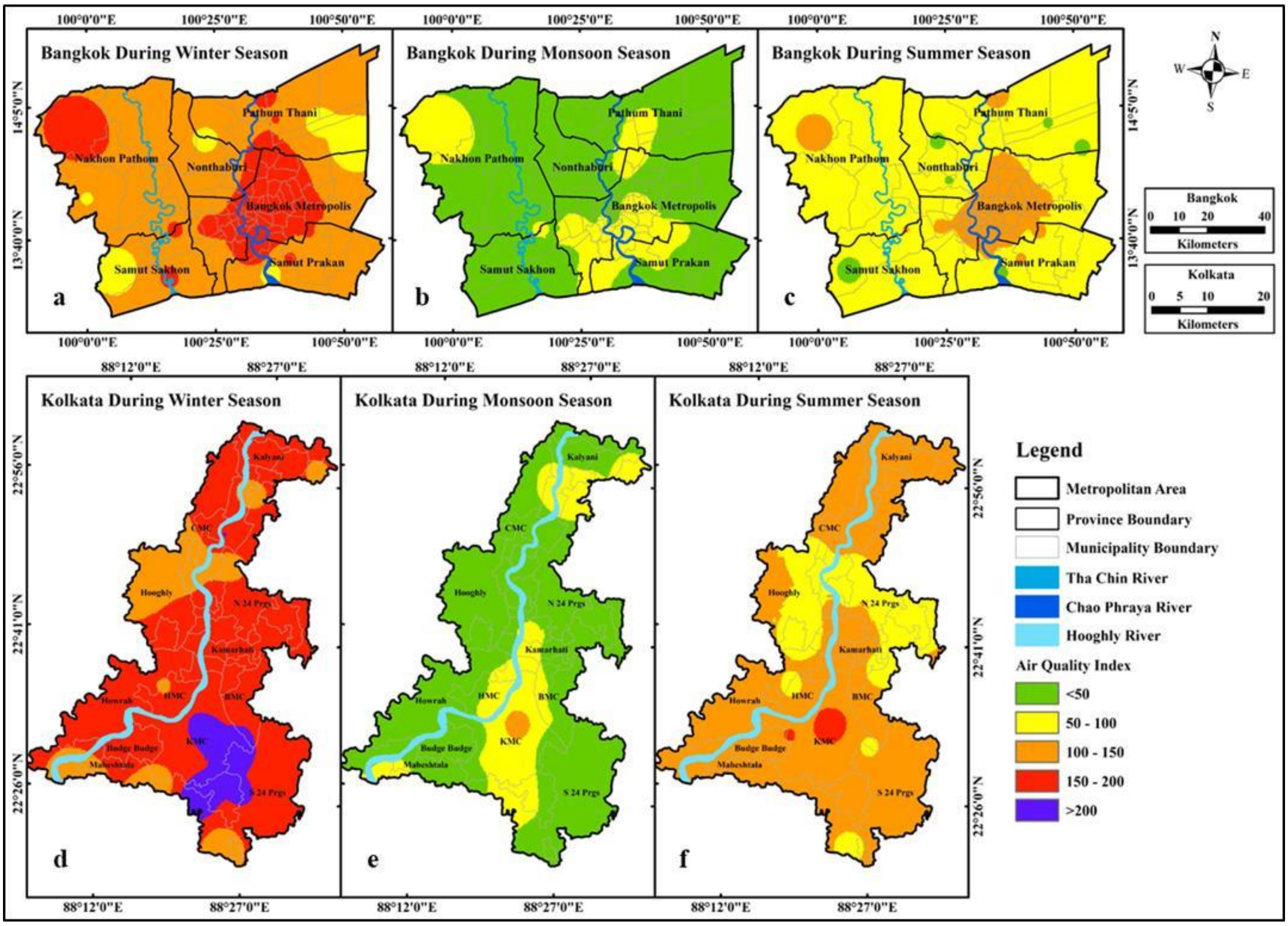

Figure 4. AQI of BMR and KMA in each season

5.1.1.3 LST:

In the BMR, during winter, the figure 6a displays about 42.11% of the area experienced temperatures between 20°C and 25°C, which covered the central region Bangkok Metropolis along with Samut Prakan in the southeast and Nakhon Pathom in the west, and the remaining region about 57.88% experience temperature below 20°C. Figure 6b, portrays, in the central region Bangkok Metropolis and parts of Samut Prakan in the southeast, about 9.97% had high temperatures during monsoon; remaining areas of about 90.03% had temperatures between 25°C and 30°C, which fall under the moderate temperature range. Figure 6c, shows very high temperature range during summer, about 29.11% of the area in the central and western areas in BMR and Nakhon Pathom shows the very high temperature range above 35°C, while about

59.11% of the area remained highly vulnerable temperature range 30°C -35°C and the rest about 11.2% gets moderately temperature of 20°C -25°C.

Figure 6d, during the winter seasons, approximately 81.32% of the areas in KMA monitored temperatures below 20°C, which are considered to be in the very low range. However, the rest 18.68% of the area in the central KMC area witnessed temperatures between 20°C and 25°C, characterizing it to be within the low range. Figure 6e shows the temperature during monsoon, about 9.12% of the area falls under the high-temperature range of 30°C to 35°C and includes the central KMC area. The remaining areas about 90.88% are in the temperature category between 25°C and 30°C, falling under the moderate range. Figure 6f shows that during summer, about 21.11% of the area was exposed to very high temperatures that went beyond 35°C in the central part of KMC along with the Kamarhati-BMC in the northeastern region, along with Kalyani in the north, and HMC in the western region, placing them in the very high-temperature range. Temperatures were between 30°C and 35°C for the remaining regions of about 78.89%, considered under the high-temperature range.

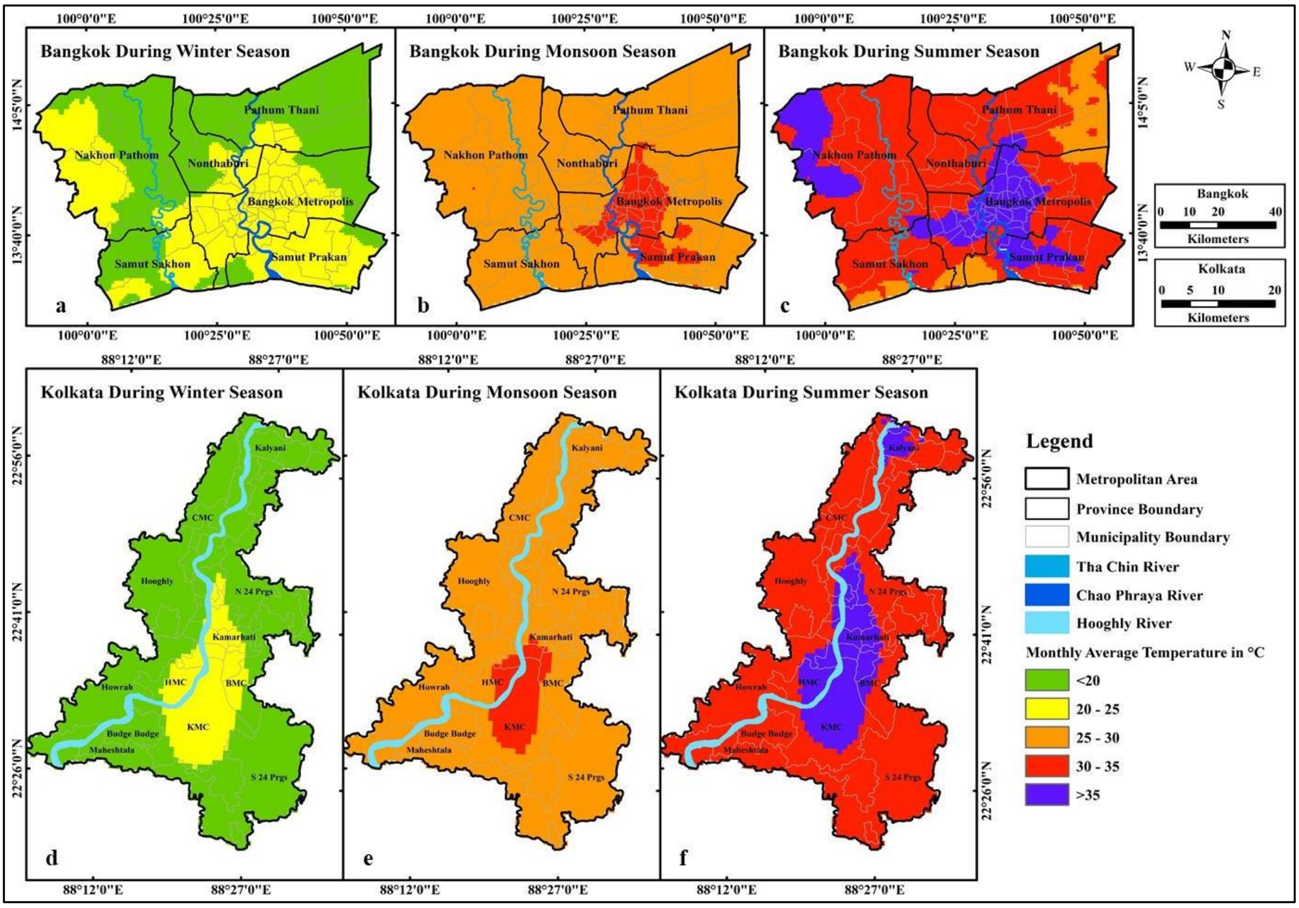

Figure 5. Monthly Average Temperature (^{O}C) of BMR and KMA in each season

5.1.2 *Exposure*

5.1.2.1 NDBI:

In BMR, the NDBI range lies within the low to highly vulnerable range as displayed in the figure 7b. In the central region of Bangkok Metropolis, Samut Prakan in the southeast region along with Nakhon Pathon in the western region about 37% of the area shows the high range of building density. About 22-26% of the area along the river Chao Phraya shows moderate range of building density. The remaining regions vary in between low to moderate range of building density.

Figure 7e represents the NDBI of KMA which varies between the moderately to the highly vulnerable range. About 23% of the area including the central region KMC, northern region North 24 Parganas, and Howrah on the western part along with the banks of the river Hooghly shows high building density. The remaining area of about 30% -34% areas including South 24 Parganas, Maheshtala, and Budge Budge in the south shows a moderately vulnerable range in building density.

5.1.2.2 NDVI:

In BMR, the figure 7a shows about 3% of the area in the southeastern region of Samut Sakhon, the southeastern region of Samut Prakan and parts of Nakhon Pathom in the western region along the central region BMR shows low vegetation index range. The areas about 31% in the eastern region Nakhon Pathom shows a high vegetation index. The remaining region about 22%-27% of the area varies vegetation in between high to moderate vegetation index range.

Figure 7d, illustrates that the NDVI in KMA lies within the moderate to low vegetation index range. About 24% of the area in the western region of Hooghly shows a high vegetation index range. In the central region KMC, the western region Howrah, and along the banks of the river Hooghly about 26% of the area shows low vegetation index. The remaining region about 30%-35% of the area presents moderate vegetation.

5.1.2.3 Population Density:

Figure 7c also illustrates the population density of BMR, particularly the central region of Bangkok Metropolis, shows the population density of about 10,000-15000. In addition, the central area has an extremely high population density of >15000. Moving to the area of Nonthaburi in the western area and Samut Prakan in the southern area, shows moderate range of population density of about by 5000-10000 and its surroundings show less range of population density of about 2000-5000 approximately. Lastly, the outer region of the BMR reflects a very low range of population density of <2,000.

Figure 7f shows KMA's population density. In the KMC central region and the western region HMC, where areas along the banks of the Ganga River show a very high population density of

>15000. Besides in the northern region North 24 Parganas and Baruipur in the southern region, along with Bally in the western region and CMC and its surroundings in the northwestern region, have a high population density ranging between 10,000 and 15000. Further, areas of BMC in the northeastern region and Howrah in the west region and Kalyani in the northern region, oscillates between medium population densities of 5000-10000. In the eastern part, Hooghly and its surroundings, along with parts of North 24 Parganas in the northern part have a low population density varying within 2,000-5,000. The southern part, consisting of South 24 Parganas along with Maheshtala, has a very low population density of <2,000.

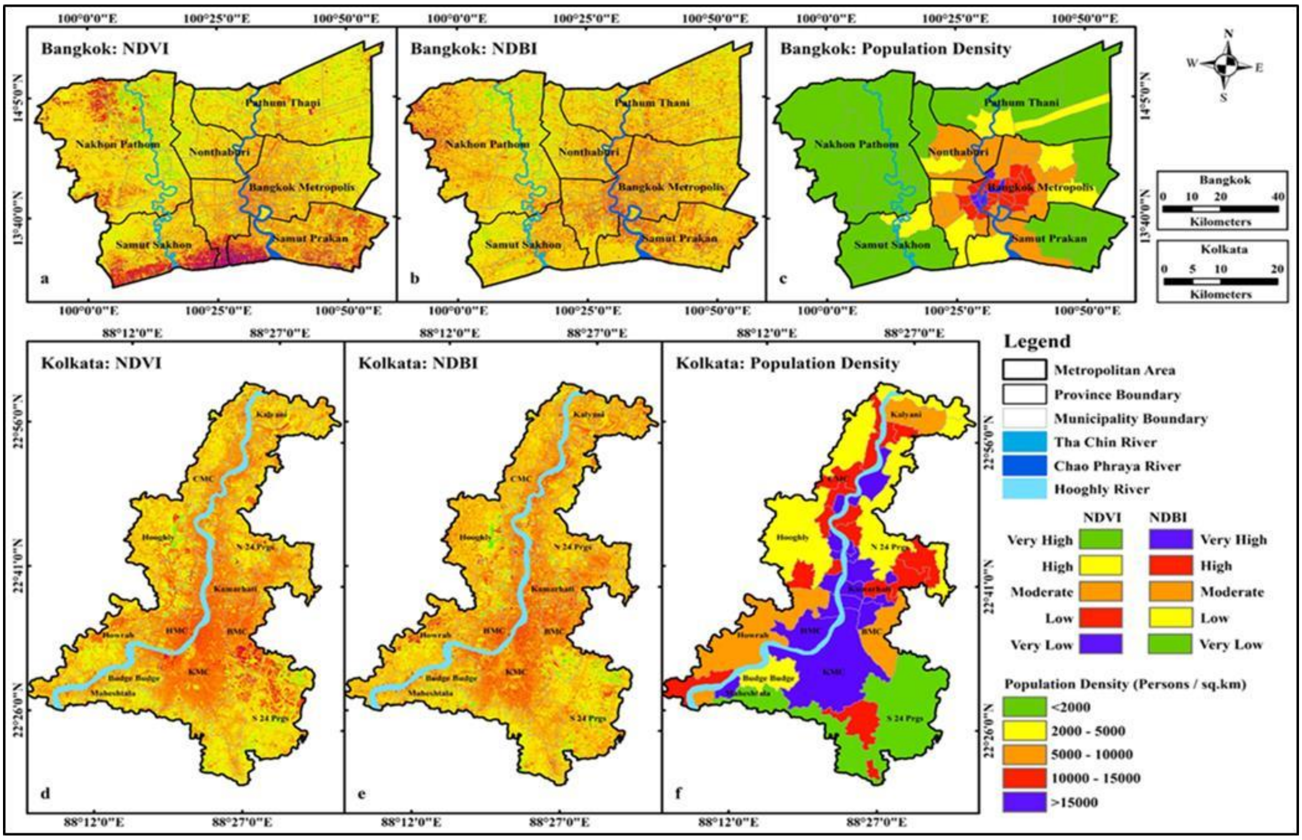

Figure 6. (a) NDVI of BMR, (b) NDBI of BMR, (c) Population Density of BMR, (d) NDVI of KMA, (e) NDBI of KMA, and (f) Population Density of KMA

5.1.3 *Vulnerability*

5.1.3.1 Old/Child Population:

Figure 8c, presents the percentage of the Old/Child Population in BMR, it displays that the percentage of the Old/Child Population varies in between 30% - 35% which is much less as compared to KMR.

Figure 8f, presents the percentage of the Old/Child Population in KMA. The map illustrates in the western region Hooghly - CMC, and Nadia and Kalyani in the north have a less Old/Child Population percentage below 35%. Furthermore, Howrah in the western region shows a moderate Old/Child Population percentage of 35% - 40%. Lastly, the central region KMC and North 24 Parganas in the north has the highest Old/Child Population percentage of >45%.

5.1.4 *Emergency Response*

5.1.4.1 Literacy Rate:

The figure 8a, illustrates the percentage of literacy rate of BMR as per the Statistical Report of Thailand published in 2021. The picture portrays a high literacy rate above 90% throughout the city and its periphery. Figure 8d, presents the literacy rate of KMA. In the northern region Nadia and in the southern region South 24 Parganas shows less literacy rate of below 80% which is said to be less as compared to other districts of KMA. Furthermore, in the western region Howrah, and North 24 Parganas - Kalyani in the north including the central region KMC shows the moderate literacy rate of 80%-90%. Lastly, in Hooghly and in the North Barrackpore-Gayespur-Dum Dum and its surroundings in the north has the highest literacy rate >90%.

5.1.4.2 Per Capita Income:

In contrast figure 8b, presents the per capita income of BMR, the central region Bangkok Metropolis has a high per capita income above 1500 USD. The northern region Nonthaburi has a moderate per capita income of 1000-1500 USD. Lastly, the remaining area has a low per capita income below 1000 USD. Figure 8e, presents the per capita income of KMA, the central region KMC has a high per capita income above 1500 USD. The eastern region BMC and western region HMC has a moderate per capita income of 1000-1500 USD. Lastly, the remaining area has a low per capita income below 1000 USD.

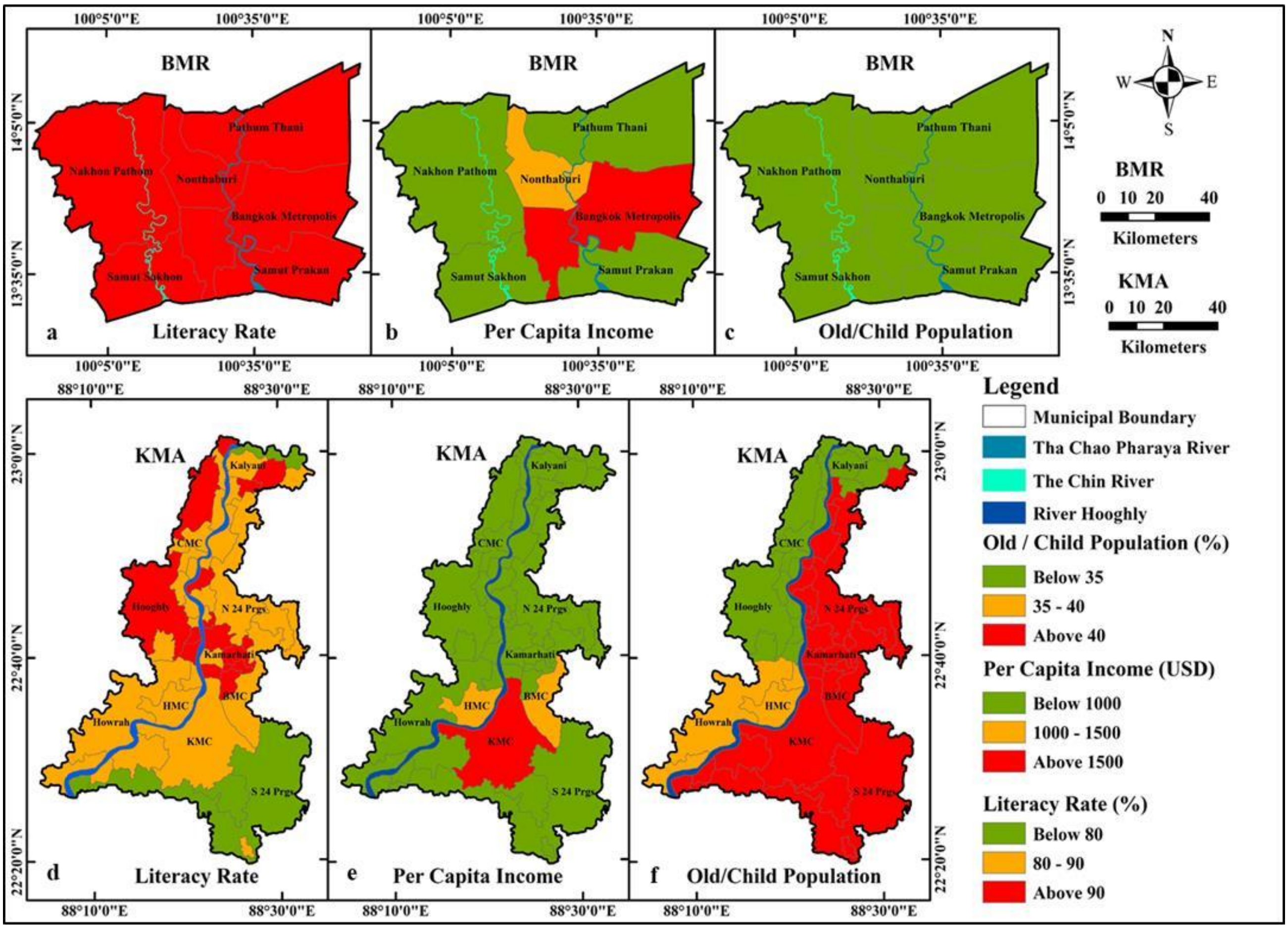

Figure 7. (a) Literacy Rate of BMR, (b) Per Capita Income of BMR, (c) Old/Child Population of BMR, (d) Literacy Rate of KMA, (e) Per Capita Income of KMA, and (f) Old/Child Population of KMA

5.1.5 *Relationship among the variables*

Before constructing the Urban Vulnerability Risk Index (UVRI) model, we evaluated the significance between the parameters in order to deeper understanding of their relationship. The correlation coefficients present the quantitative measures that indicate the significant relationship between two variables and their nature and magnitude (+/-). We perform the Spearman correlation coefficient test to establish the relationship between two parameters. The Spearman correlation evaluates the relationship between the variables when the function consistently increases or decreases but may not be linear.

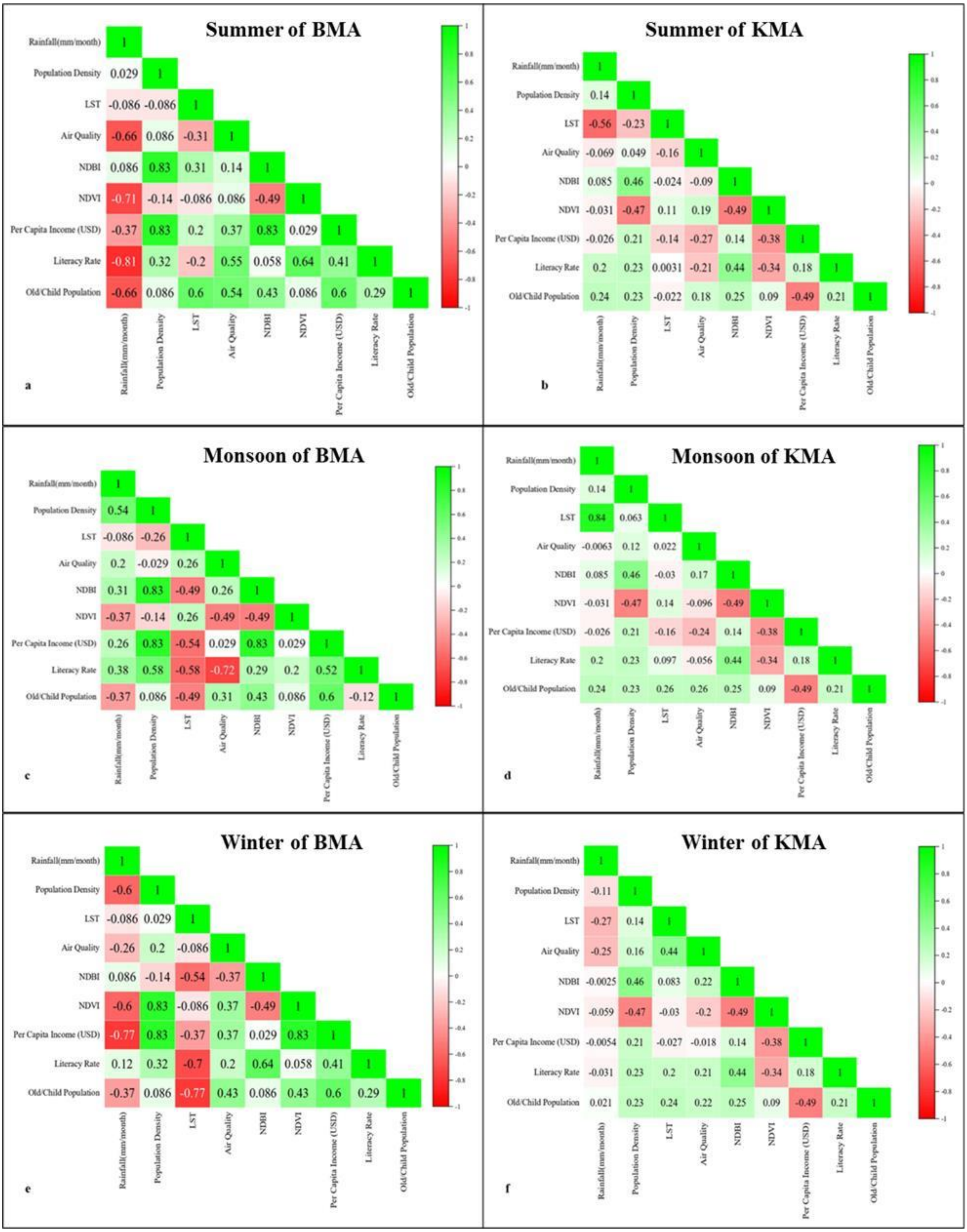

Figure 8. Spearman correlation coefficient plot of the study area in different seasons

During summer months in BMR, LST shows a significant positive correlation with the Old/Child Population of (0.6), which signifies that areas with higher temperatures may have a probability of higher elderly and children population groups, making them more susceptible to vulnerability and also a weakly positive correlation with NDBI (0.31) indicates that areas with higher impervious surface and high building density inclined to have a higher temperature, and a weakly negative correlation with AQI (-0.31) implies that higher temperature may responsible for dispersion of air pollutants which leads to better air quality. In contrast, during the summer months in KMA, the negative correlation between LST and rainfall (-0.56) signifies that areas with higher temperatures get less rainfall, due to the generation of Urban Heat Island (UHI) effect.

During monsoon months in BMR, rainfall has a significant positive correlation with Population density (0.54) implies that areas with higher population receives more rainfall during monsoon due to urban infrastructures and microclimate and improper drainage system is responsible for urban flooding due to heavy rainfall, a weak correlation with NDBI (0.31) interprets that high built up areas experience more rainfall due to urban induced rainfall effects such as tiny particles (aerosols) formed from pollution acts as a source of cloud formation, and change in wind pattern due to high risers alters the distribution and movement of rainclouds, hence receives high rainfall and also weakly correlate with Literacy Rate (0.38) implies that areas with higher literacy rates have proper urban management plan to cope up with heavy rainfall and thus are less susceptible to urban flooding, and a weakly negative correlation with NDVI (-0.37) indicates that areas with less green space due to urban sprawl receives more rainfall due to urban induced effects and also a weakly negative correlation with Old/Child population (-0.37) indicates that waterlogging due to heavy rainfall increases the chances of waterborne diseases such *Dengue-Malaria-Typhoid* and many more. Similarly, in KMA, rainfall has a positive correlation with LST (0.84) interpretes that the complex relationship between temperature and rainfall, higher temperature increases the humidity in the environment, and urban nature, topography, Land Use Land Cover (LULC) pattern also plays an important role in this condition.

In winter AQI of BMR shows a significant positive correlation with the Old/Child Population (0.43) indicates higher AQI increases the chances of cardiovascular diseases, neurological diseases, and asthma, particularly to these demographic groups, heightened the risk of vulnerability, and also shows weakly positive correlation with NDVI (0.37) indicates more the green space or open areas has better air quality and Per capita Income (0.37) implies that higher income groups tend to have less vulnerability to air quality as they might have proper precautions and management planning to cope up and negatively correlates with NDBI (-0.37) shows that construction areas and high building density are prone to highly vulnerable to air quality as concrete and other building materials produce tiny particles which are responsible for the worsening of the air quality.

5.1.6 *Urban Vulnerability Index (UVI) Modelling*

5.1.6.1 Bangkok Metropolitan Region (BMR)

Figure 10, portrays the Urban Vulnerability Index of BMR in different seasons. In monsoon about 42.1% of the area in the northern region of Pathum Thani and Nakhon Pathom in the northwestern region lies in the low vulnerable (0-5) range and about 19.22% of the area has low to moderate vulnerable (5-6) range. About 27.30% of the area surrounding the central region and western region of Nakhon Pathom along with the eastern region in the Pathum Thani, and Samut Prakan in the southeast lies in the moderately vulnerable (6-7) range. Areas of about 12.08% in the outer region of the metropolis show a moderate to high vulnerable (7-8) range and 37.3% (585.237 sq. km.) of the area in the central region has the highest vulnerable range (8-10). In contrast, during summer about 49.3% of the area in southwest Samut Sakhon, in west Nakhon Pathom, and the outer region of Pathum Thani in the east has low to moderate vulnerable (5-6) range. About 18.71% of the area in west Nakhon Pathom and the outer region of the metropolis has a moderately vulnerable (6-7) range and about 7.07% of the area along the Chao Phraya River in the central region is considered as moderate to high vulnerable (7-8) range. About 0.3% (4.702 sq. km.) area of the central region has the highest vulnerable range (8-10). Lastly, during winter about 64.3% area in west Nakhon Pathom, Pathum Thani in the east, and southwest Samut Sakhon lies in the low vulnerable (0-5) range, and about 14.69% of the area has low to moderate vulnerable (5-6) range. About 16.54% area is in the outer region of the central area, and in west Nakhon Pathom has a moderately vulnerable (6-7) range. The central region of about 4.44% area has a moderate to high vulnerable (7-8) range. So, the overall Urban Vulnerability Index (UVI) of BMR is monsoon > summer > winter.

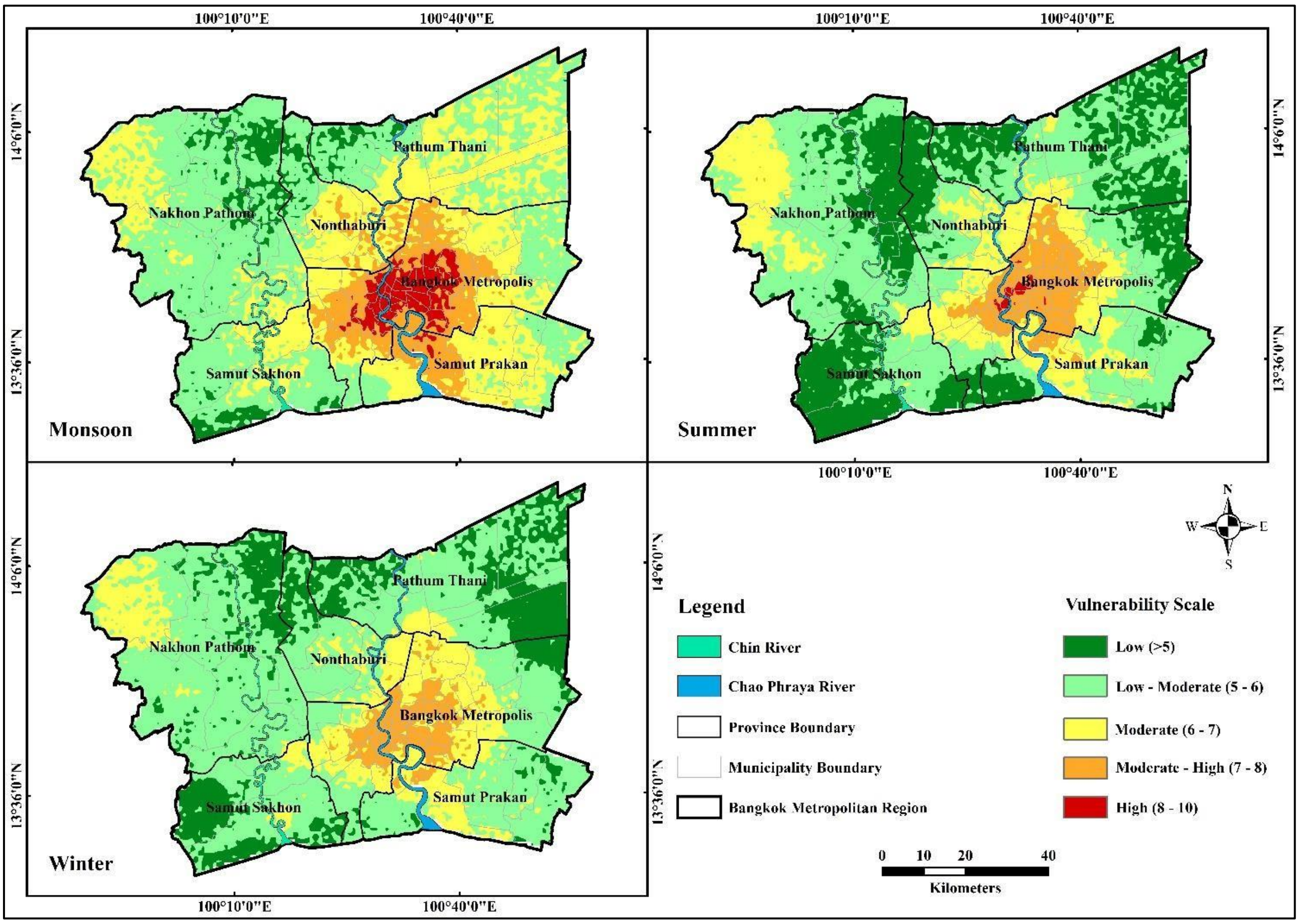

Figure 9. Urban Vulnerability Index of BMR during each season

5.1.6.2 Kolkata Metropolitan Area (KMA)

Figure 11, portrays the Urban Vulnerability Index of KMA in different seasons. In monsoon is much more vulnerable followed by the summer and winter seasons. After the analysis, figure 11 illustrates that during monsoon about 3.34% of the area towards Hooghly in the western region is in the less vulnerable (0-5) range, and 50.09% of the area is in the low to moderate vulnerable (5-6) range. Correspondingly, 25.18% of the area in the eastern and western region lies in the moderately vulnerable (6-7) range, and about 17.77% area along the banks of the river Hooghly and in the southern region has a moderate to high vulnerable (7-8) range and about 3.62% (68.297 sq. km.) of the area in the central region lies in highly vulnerable (8-10) zone. In summer about 5.7% of the area in the western and southern regions has a low vulnerable (0-5) range and about 60.39% of the area lies in a low to moderate vulnerable (5-6) range. The eastern region along the surroundings of the city centre shows about 11.4% of the area is in the moderately vulnerable (6-7) range. In the central region, about 1.14% (21.50 sq. km.) of the area is in a highly vulnerable (8-10) zone. During winter, about 20.74% of the area is majorly distributed in the western region, and parts in the eastern region, and southern region have the less vulnerable (0-5) range and in the outer region of KMA, about 20.74% of the area lies in the low to moderate vulnerable (5-6) range. About 19.77% of the areas along the banks of the river Hooghly show the moderately vulnerable (6-7) range. Lastly, about 3.06% of the area in the central region of KMC shows a moderate to high vulnerable (7-8) range. So, the overall Urban Vulnerability Index (UVI) of KMA is monsoon > summer > winter.

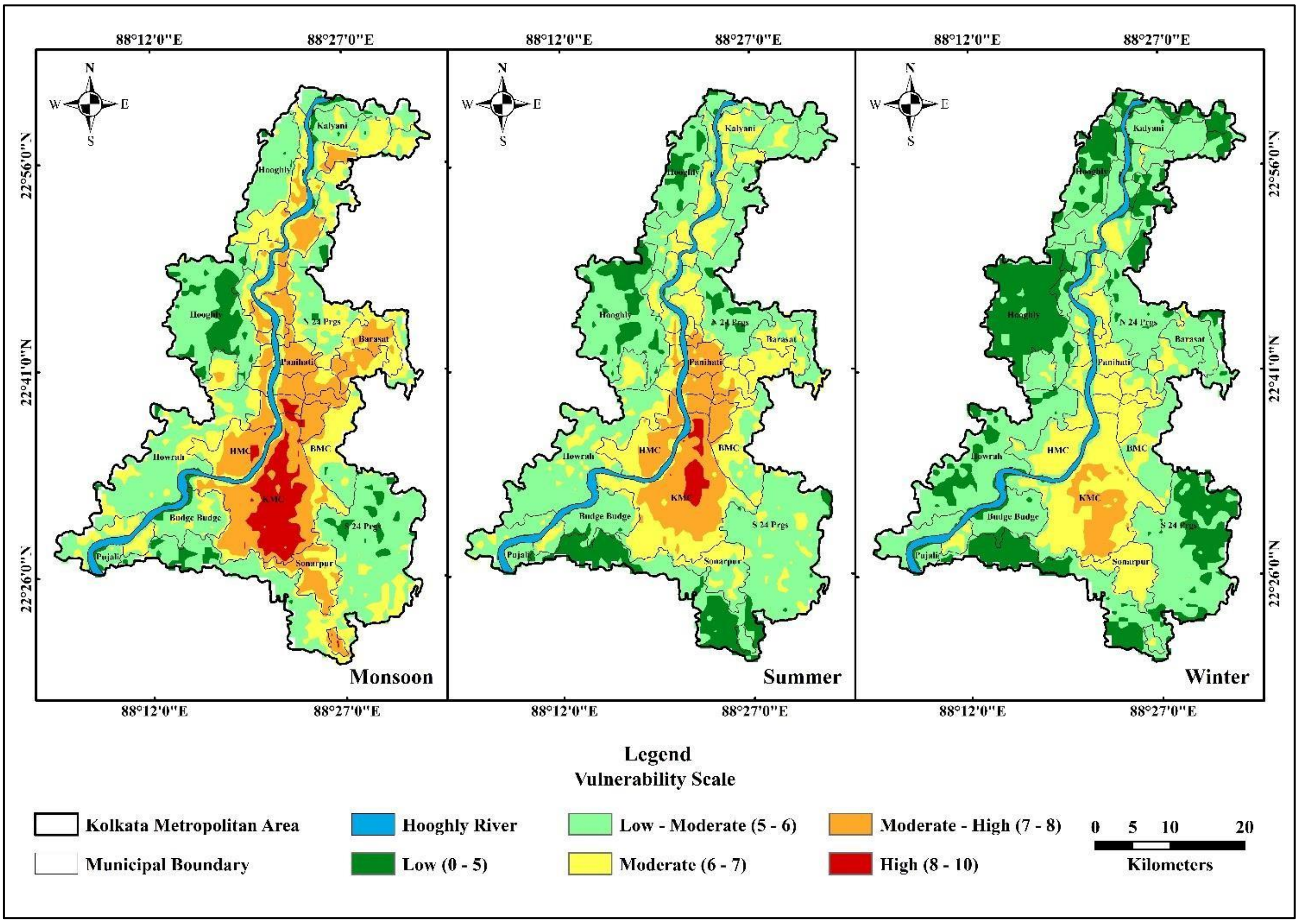

Figure 10. Urban Vulnerability Index of KMA during each season

5.2 *Discussion*

The vulnerability assessment has dominated climate change adaptation programs at various levels of community, city, region, country, and the world entirely. The Vulnerability Index of this study represents that the centre of the city and its surroundings of both the study area is highly exposed to urban vulnerability as the urban areas have high impervious surface, congested and densely populated. In monsoon, the central region of Kolkata Municipality of KMA and Bangkok Metropolis of BMR is much more vulnerable than the surrounding outer region because of the heavy rainfall along with high building density and impoper drainage management. As a result, urban flooding occurs which leads to disruption in transportation, damage of properties, and health and hygiene issues. In contrast, during summer the metropolis is highly vulnerable to high temperature as compare to surrounding areas of KMA and BMR because of impervious surfaces and lack of green spaces. To meet the requirement of the urban sprawl, in the metropolis the impervious surface increases in space of green areas, which generate Urban Heat Island (UHI) effect, primarily responsible for the heatwaves in the city. Due to excessive heatwaves in the city, concentrations of air conditioners are increasing day by day, which has a negative impact in the environment. As air conditioners remove the heat from the inside of the building and release it to the outdoor environment, this expels heat and thus, contributing to an increase in temperature, especially in densely populated areas. Traffic congestion releases an immense amount of heat into the surrounding environment, especially during peak hours. On the other hand, during winter, the central region observe worsened air quality because the dry climate and industrial belts are situated in nearby areas as well as heavy traffic that emit notable amounts of pollutants like So_x and No_x, $PM_{2.5}$, and PM_{10}. These environmental hazards heightened the risk of vulnerability to the elderly and children population, they may get affected by severe disease and increase the chance of mortality. However, highly literate areas and high-income groups tend to be less susceptible to environmental hazards, as they have proper management systems and precautions in place to deal with such situations.

Chapter 6: Conclusion

6 Conclusion

In this study, we evaluated climate justice in the Kolkata Metropolitan Area and Bangkok Metropolitan Region by analyzing significant spatial variability in the context of Urban Vulnerability. The study also highlights that socio-economic and demographic parameters like population density, old/child population, literacy rate, and income levels, as well as environmental parameters like LST, AQI, and rainfall, interact effectively to influence urban vulnerability.

In summer due to high temperatures and UHI effect heat waves are generated, which trigger the probability of heatstroke, cardiovascular diseases, neurological diseases and increase mortality rates, reduce productivity, and deplete the groundwater level. In monsoons, heavy rainfall increases the chances of urban flooding, which disrupts the water and sanitation system, leading to severe traffic congestion and closure of the key routes disrupting daily life, damaging public properties including roads, bridges, and railway lines, increasing waterborne diseases such as *Malaria, Dengue* and many more. In winter, poor AQI leads to severe diseases such as *Chronic Obstructive Pulmonary Disease* (COPD), increases the chances of cancer, asthma, and bronchitis, and also affects children's immune systems, similarly elderly population is at high risk of severe health issues due to poor AQI and increase the number of premature mortality.

The central region and eastern region of KMA and BMR are exposed to significant heat, rainfall and air pollution making home to the most vulnerable population due to the proximity to industrial belts, higher urbanization rates and the influence of local climate. The increased in the concrete area by sacrificing green spaces generated the Urban Heat Island (UHI) effect, which is responsible for worsening of AQI and increasing in temperature as the concrete area has a tendency to absorb and retain heat. Areas with low-income levels and literacy rates are tend to much more vulnerable as compared to others. This study also reflects that particularly the old/child population are vulnerable because this demographic groups are highly exposed to adverse effects of environments such as extreme temperatures, poor air quality, heavy rainfall and inadequate infrastructure.

The findings of this study highlight the need of proper implications for urban planning and disaster management in both the regions. The policymakers should focus on building adaptive strategies which addresses the specific vulnerabilities identified in the center of the city and in the eastern region of both the metropolis. The old and child population should get attention by improving infrastructure resilience, betterment of the healthcare facilities and by implementing proper environmental regulations to control industrial and vehicular emission.

In addition, future research could extent upon this study by employing machine learning algorithms to further refine Urban Vulnerability of the metropolis. Similarly, comparative studies with other delta region could provide a broader perspective in understanding of the Urban Vulnerability in the context of climate change and urban sprawl. In conclusion, the application of the GIS based Fuzzy MCDA technique has been proven to be a useful tool for determining and understanding urban vulnerability in complex urban areas. The study not only sheds light to the ongoing challenges faced by the Hooghly River deltas and Chao Pharaya River Delta but also offers a foundation for future research and policy development, focused at promoting resilient and sustainable environment.

References

Angel, S., Parent, J., Civco, D. L., Blei, A. & Potere, D. Te dimensions of global urban expansion: Estimates and projections for all countries 2000–2050. Dimens. Glob. Urban Expans. Estim. Proj. Ctries. 75, 53–107 (2011).

Ashfaq, M., Shi, Y., Tung, W., Trapp, R.J., Gao, X., Pal, J.S., Diffenbaugh, N.S., 2009. Suppression of South Asian summer monsoon precipitation in the 21st century. Geophysical Research Letters 36, L01704. http://dx.doi.org/10.1029/ 2008GL036500.

Bose, S. and Mazumdar, A., 2023. Urban flood risk assessment and mitigation with InVEST-UFRM model: a case study on Kolkata city, West Bengal state (India). *Arabian Journal of Geosciences*, *16*(5), p.320.

Bren d'Amour, C., Reitsma, F., Baiocchi, G., Barthel, S., Güneralp, B., Erb, K.H., Haberl, H., Creutzig, F. and Seto, K.C., 2017. Future urban land expansion and implications for global croplands. *Proceedings of the National Academy of Sciences*, *114*(34), pp.8939-8944.

Chakraborty, S., Maity, I., Patel, P.P., Dadashpoor, H., Pramanik, S., Follmann, A., Novotny, J., Roy, U., 2021b. Spatio-temporal patterns of urbanization in the Kolkata Urban Agglomeration: a dynamic spatial territory-based approach. Sustain. Cities Soc. 67, 102715. https://doi.org/10.1016/j.scs.2021.102715.

Chen, D., & Brutsaert, W. (1998). Satellite-sensed distribution and spatial patterns of vegetation parameters over a tallgrass prairie. Journal of the Atmospheric Sciences, 55(7), 1225–1238.

Chitwatkulsiri, D., Miyamoto, H. and Weesakul, S., 2021. Development of a simulation model for real-time urban floods warning: a case study at Sukhumvit Area, Bangkok, Thailand. *Water*, *13*(11), p.1458.

Crippa M et al (2018) Gridded emissions of air pollutants for the period 1970–2012 within EDGAR v4.3.2. Earth System Sci Data 10(4):1987–2013

Cutter, S.L., 2016. The changing context of hazard extremes: Events, impacts, and consequences. *Journal of Extreme Events*, *3*(02), p.1671005.

Doblas-Reyes, F. J,. A. A. Sörensson, M. Almazroui, A. Dosio, W. J. Gutowski, R. Haarsma, R. Hamdi, B. Hewitson, W-T. Kwon, B. L. Lamptey, D. Maraun, T. S. Stephenson, I. Takayabu, L. Terray, A. Turner, Z. Zuo, 2021, Linking Global to Regional Climate Change. In: Climate Change 2021: The Physical Science Basis. Contribution of Working Group I to the Sixth Assessment Report of the Intergovernmental Panel on Climate Change [Masson-Delmotte, V., P. Zhai, A. Pirani, S. L. Connors, C. Péan, S. Berger, N. Caud, Y. Chen, L. Goldfarb, M. I. Gomis, M. Huang, K. Leitzell, E. Lonnoy, J.B.R. Matthews, T. K. Maycock, T. Waterfield, O. Yelekçi, R. Yu and B. Zhou (eds.)]. Cambridge University Press. In Press.

Dodman, D., B. Hayward, M. Pelling, V. Castan Broto, W. Chow, E. Chu, R. Dawson, L. Khirfan, T. McPhearson, A. Prakash, Y. Zheng, and G. Ziervogel, 2022: Cities, Settlements and Key Infrastructure. In: Climate Change 2022: Impacts, Adaptation and Vulnerability. Contribution of Working Group II to the Sixth Assessment Report of the Intergovernmental Panel on Climate Change [H.-O. Pörtner, D.C. Roberts, M. Tignor, E.S. Poloczanska, K. Mintenbeck, A. Alegría, M. Craig, S. Langsdorf, S. Löschke, V. Möller, A. Okem, B. Rama (eds.)]. Cambridge University Press, Cambridge, UK and New York, NY, USA, pp. 907–1040, doi:10.1017/9781009325844.008

Duan, C., Zhang, J., Chen, Y., Lang, Q., Zhang, Y., Wu, C. and Zhang, Z., 2022. Comprehensive risk assessment of urban waterlogging disaster based on MCDA-GIS integration: The case study of Changchun, China. *Remote Sensing*, *14*(13), p.3101.

Filho WL et al (2021) Addressing the urban heat islands effect: A cross-country assessment of the role of green infrastructure. Sustainability 13:753

Gabriel, K.M.A.; Endlicher, W.R. Urban and rural mortality rates during heat waves in Berlin and Brandenburg, Germany. Environ. Pollut. 2011, 159, 2044–2050.

Gillies, R. R., Kustas, W. P., & Humes, K. S. (1997). A verification of the 'triangle' method for obtaining surface soil water content and energy fluxes from remote measurements of the Normalized Difference Vegetation Index (NDVI) and surface e. International Journal of Remote Sensing, 18(15), 3145–3166. https://doi.org/ 10.1080/014311697217026.

Gracey, M., 2002. Child health in an urbanizing world. *Acta Paediatrica*, *91*(1), pp.1-8.

Groce, N.; Bellamy, R.; Wolff, J. Managing the health effects of climate change: Lancet and University College London Institute for Global Health Commission. Lancet. 2009, 373, 1693–1733.

Guhathakurta, P., Sreejith, O.P. and Menon, P.A., 2011. Impact of climate change on extreme rainfall events and flood risk in India. *Journal of earth system science, 120*, pp.359-373.

Gurjar, B.R., Ravindra, K. and Nagpure, A.S., 2016. Air pollution trends over Indian megacities and their local-to-global implications. *Atmospheric Environment*, *142*, pp.475-495.

Hasnine, M., Rukhsana Modelling of sustainable and suitable land selection for future urban development: a study around Kolkata city, India. *Arab J Geosci* **16**, 504 (2023). https://doi.org/10.1007/s12517-023-11607-7

Hess, J.J.; McDowell, J.Z.; Luber, G. Integrating climate change adaptation into public health practice: Using adaptive management to increase adaptive capacity and build resilience. Environ. Health Perspect. 2012, 120, 171–179. [CrossRef] [PubMed]

Huang, X., Hao, L., Sun, G., Yang, Z.L., Li, W. and Chen, D., 2022. Urbanization aggravates effects of global warming on local atmospheric drying—Geophysical *Research Letters*, *49*(2), p. e2021GL095709.

IPCC. 2021. Climate Change 2021: The Physical Science Basis. Contribution of Working Group I to the Sixth Assessment Report of the Intergovernmental Panel on Climate Change. V. Masson-Delmotte, P. Zhai, A. Pirani, S.L. Connors, C. Péan, S. Berger, N. Caud, Y. Chen, L. Goldfarb, M.I. Gomis, M. Huang, K. Leitzell, E. Lonnoy, J.B.R. Matthews, T.K. Maycock, T. Waterfield, O. Yelekçi, R. Yu and B. Zhou, (eds.). Cambridge, Cambridge University Press. www.ipcc.ch/report/ar6/wg1/downloads/report/IPCC_AR6_WGI_Full_Report.pdf

Lelieveld, J., Evans, J.S., Fnais, M., Giannadaki, D. and Pozzer, A., 2015. The contribution of outdoor air pollution sources to premature mortality on a global scale. *Nature*, *525*(7569), pp.367-371.

Liu, K., Su, H., Li, X., Wang, W., Yang, L. and Liang, H., 2016. Quantifying spatial–temporal pattern of urban heat island in Beijing: An improved assessment using land surface temperature (LST) time series observations from LANDSAT, MODIS, and Chinese new satellite GaoFen-1. *IEEE Journal of Selected Topics in Applied Earth Observations and Remote Sensing*, *9*(5), pp.2028-2042.

Maity, S., Das, S., Pattanayak, J.M., Bera, B. and Shit, P.K., 2022. Assessment of ecological environment quality in Kolkata urban agglomeration, India. *Urban Ecosystems*, *25*(4), pp.1137-1154.

Maji, K.J., Arora, M. and Dikshit, A.K., 2017. Burden of disease attributed to ambient PM 2.5 and PM 10 exposure in 190 cities in China. *Environmental Science and Pollution Research*, *24*, pp.11559-11572.

Malik, S., Pal, S.C., Sattar, A., Singh, S.K., Das, B., Chakrabortty, R. and Mohammad, P., 2020. Trend of extreme rainfall events using suitable Global Circulation Model to combat the water logging condition in Kolkata Metropolitan Area. *Urban Climate*, *32*, p.100599.

Marks, D., Connell, J. and Ferrara, F., 2020. Contested notions of disaster justice during the 2011 Bangkok floods: Unequal risk, unrest and claims to the city. *Asia Pacific Viewpoint*, *61*(1), pp.19-36.

Mirzaei, M., Verrelst, J., Arbabi, M., Shaklabadi, Z. and Lotfizadeh, M., 2020. Urban heat island monitoring and impacts on citizen's general health status in Isfahan metropolis: A remote sensing and field survey approach. *Remote Sensing*, *12*(8), p.1350.

Mukherjee, A.B. and Bardhan, S., 2021. Flood vulnerability and slum concentration mapping in the Indian city of Kolkata: A post-Amphan analysis. *Water Science*, *35*(1), pp.109-126.

Naik, V., S. Szopa, B. Adhikary, P. Artaxo, T. Berntsen, W. D. Collins, S. Fuzzi, L. Gallardo, A. Kiendler Scharr, Z. Klimont, H. Liao, N. Unger, P. Zanis, 2021, Short-Lived Climate Forcers. In: Climate Change 2021: The Physical Science Basis. Contribution of Working Group I to the Sixth Assessment Report of the Intergovernmental Panel on Climate Change [Masson-Delmotte, V., P. Zhai, A. Pirani, S. L. Connors, C. Péan, S. Berger, N. Caud, Y. Chen, L. Goldfarb, M. I. Gomis, M. Huang, K. Leitzell, E. Lonnoy, J. B. R. Matthews, T. K. Maycock, T. Waterfield, O. Yelekçi, R. Yu and B. Zhou (eds.)]. Cambridge University Press. In Press.

Nishadh, K.A., Azeez, P.A. and Mohanraj, R., 2015. Real-time air pollution modeling and dissemination of location-based information using mobile devices.

Ometto, J.P., K. Kalaba, G.Z. Anshari, N. Chacón, A. Farrell, S.A. Halim, H. Neufeldt, and R. Sukumar, 2022: CrossChapter Paper 7: Tropical Forests. In: Climate Change 2022: Impacts, Adaptation and Vulnerability. Contribution of Working Group II to the Sixth Assessment Report of the Intergovernmental Panel on Climate Change [H.-O. Pörtner, D.C. Roberts, M. Tignor, E.S. Poloczanska, K. Mintenbeck, A. Alegría, M. Craig, S. Langsdorf, S. Löschke, V. Möller, A. Okem, B. Rama (eds.)]. Cambridge University Press, Cambridge, UK and New York, NY, USA, pp. 2369–2410, doi:10.1017/9781009325844.024.

Pakarnseree, R., Chunkao, K. and Bualert, S., 2018. Physical characteristics of Bangkok and its urban heat island phenomenon. *Building and Environment*, *143*, pp.561-569.

Patil, D.G. and Kashid, S.S., 2023, August. Review on Resilient Spatial Planning Strategies to Reduce Urban Flood Risks Check for updates. In *Flood Forecasting and Hydraulic Structures: Proceedings of 26th International Conference on Hydraulics, Water Resources and Coastal Engineering (HYDRO 2021)* (Vol. 340, p. 217). Springer Nature.

Peng, C.; Zhang, J.; Zhang, L.; Sun, Y. Evaluation of Resident Evacuations in Urban Rainstorm Waterlogging Disasters Based on Scenario Simulation: Daoli District (Harbin, China) as an Example. Int. J. Environ. Res. Public Health 2014, 11, 9964–9980

Rezaei, H., Macioszek, E., Derakhshesh, P., Houshyar, H., Ghabouli, E., Bakhshi Lomer, A.R., Ghanbari, R. and Esmailzadeh, A., 2023. A spatial decision support system for modeling urban resilience to natural hazards. *Sustainability*, *15*(11), p.8777.

Roxy, M.K., Ghosh, S., Pathak, A., Athulya, R., Mujumdar, M., Murtugudde, R., Terray, P. and Rajeevan, M., 2017. A threefold rise in widespread extreme rain events over central India. *Nature Communications*, *8*(1), pp.1-11.

Sarraf, M., Dasgupta, S., Roy, S. and Belle, A., 2011. India-Vulnerability of Kolkata metropolitan area to increased precipitation in a changing climate.

Serreze, M.C., Barry, R.G., 2010. Climate change. In: Barry, R.G., Chorley, R.J. (Eds.), Atmosphere, Weather and Climate. Routledge, Oxon

Seto, K. C., Güneralp, B. & Hutyra, L. R. Global forecasts of urban expansion to 2030 and direct impacts on biodiversity and carbon pools. Proc. Natl. Acad. Sci. 109, 16083 (2012).

Seto, K. C., Sánchez-Rodríguez, R. & Fragkias, M. Te new geography of contemporary urbanization and the environment. Annu. Rev. Environ. Resource. 35, 167–194 (2010)

Shaw, R., Y. Luo, T.S. Cheong, S. Abdul Halim, S. Chaturvedi, M. Hashizume, G.E. Insarov, Y. Ishikawa, M. Jafari, A. Kitoh, J. Pulhin, C. Singh, K. Vasant, and Z. Zhang, 2022: Asia. In: Climate Change 2022: Impacts, Adaptation and Vulnerability. Contribution of Working Group II to the Sixth Assessment Report of the Intergovernmental Panel on Climate Change [H.-O. Pörtner, D.C. Roberts, M. Tignor, E.S. Poloczanska, K. Mintenbeck, A. Alegría, M. Craig, S. Langsdorf, S. Löschke, V. Möller, A. Okem, B. Rama (eds.)]. Cambridge University Press, Cambridge, UK and New York, NY, USA, pp. 1457–1579, doi:10.1017/9781009325844.012

Saaty T. L., 2008. Decision making with the analytic hierarchy process, *International Journal of Services Sciences.* 1(1) , pp 83-98 https://doi.org/10.1504/ijssci.2008.017590

Solecki, W., Rosenzweig, C., Blake, R., de Sherbinin, A., Matte, T., Moshary, F., Rosenzweig, B., Arend, M., Gaffin, S., Bou-Zeid, E. and Rule, K., 2015. New York City panel on climate change 2015 report chapter 6: Indicators and monitoring. *Annals of the New York Academy of Sciences*, *1336*(1), pp.89-106.

Statistical Forecasting Division, Bangkok: National Statistical Office, Thailand. Statistical Yearbook Thailand 2020. http://service.nso.go.th/nso/nsopublish/pub s/e-book/SYB-2020/18/index.html. (Accessed 18 April 2023).

Sun, Y., Chen, Y., Huang, Y., Luo, Y., Yan, L., Man, S., Yu, C., Lv, J., Wang, C., Wu, J. and Bao, H., 2024. Association of urban green space with metabolic syndrome and the role of air pollution. *Landscape and Urban Planning*, *248*, p.105100.

T. Taichi, Use of high-resolution elevation data to access the vulnerability of the Bangkok metropolitan area to sea level rise, Hydrol. Res. Lett. 14-4 (2020) 136–142, https://doi.org/10.3178/hrl.14.136.

The Hindu (2017). 31 dead, 20 lakh affected in West Bengal floods. 29 July 2017. Retrieved from https://www.the hindu.com/news/national/other-states/bengal-flood-toll reaches-31-iaf-rescues-stranded-villagers/arti cle19386721.ece, accessed on 7.10.2019.

The Urbanization of Bangkok: Its Prominence, Problems, and Prospects. Available online: https://archive.unu.edu/unupress/ unupbooks/uu11ee/uu11ee0z.htm (accessed on 6 February 2022). https://www.tei.or.th/thaicityclimate/public/work-20.pdf

Tiwari, P.C., 2000. Land-use changes in Himalaya and their impact on the plain's ecosystem: need for sustainable land use. *Land use policy*, *17*(2), pp.101-111.

United Nations Department of Economic and Social Affairs, Population Division (2022). World Population Prospects 2022: Summary of Results. UN DESA/POP/2022/TR/NO. 3.

United Nations Human Settlements Programme (UN-Habitat). World Cities Report 2022: Envisaging the future cities. (2022).

United Nations, Department of Economic and Social Affairs Highlights 2022-2023 Published by the United Nations, Department of Economic and Social Affairs New York, New York 10017, United States of America.

Vargas, N. and Magaña, V., 2020. Climatic risk in the Mexico City metropolitan area due to urbanization. *Urban Climate*, *33*, p.100644.

Weng, Q., & Lo, C. P. (2001). Spatial analysis of urban growth impacts on vegetative greenness with Landsat TM data. Geocarto International, 16(4), 19–28. https://doi. org/10.1080/10106040108542211.

WMO, 2023. Weather-Related Disasters Increase Over Past 50 Years, Causing More Damage. https://public.wmo.int/en/media/press-release/weather-relateddisasters-increase-over-past-50-years-causing-more-damage-fewer.

World Air Quality Report, 2023; by IQAir; https://www.iqair.com/dl/2023_World_Air_Quality_Report.pdf

World Population Ageing 2015. United Nations Department of Economic and Social Affairs, Population Division.

Zhang, Y., Shen, J. and Li, Y., 2018. An atmospheric vulnerability assessment framework for environment management and protection based on CAMx. *Journal of environmental management*, *207*, pp.341-354.

Zhang, Y., Shen, J., Ding, F., Li, Y. and He, L., 2016. Vulnerability assessment of atmospheric environment driven by human impacts. *Science of the Total Environment*, *571*, pp.778-790.

Zhou, W., Huang, G. and Cadenasso, M.L., 2011. Does spatial configuration matter? Understanding the effects of land cover pattern on land surface temperature in urban landscapes. *Landscape and urban planning*, *102*(1), pp.54-63.